Peer Review File

Editorial Note: some text and figures have been removed from this file to preserve confidential data

Manuscript Title: Tumor extracellular vesicles and particles dysregulate liver metabolism Reviewer Comments & Author Rebuttals

Reviewer Reports on the Initial Version:

Referee #1 (Remarks to the Author):

The study by Wang explores the systemic effects of cancer-derived extracellular vesicles and particles (EVPs), especially as inducers of fatty liver disease. This represents an aspect of systemic cancer progression unrelated to liver metastasis. The authors noted that cancer-associated liver disfunction is and important but poorly understood paraneoplastic pathology that can be recapitulated in models of transplantable murine cancers, such as B16F10 melanoma, K7M2 osteosarcoma and mammary cancers (67NR and subline of 4T1). While these tumors did not form overt liver metastases, they remotely triggered a condition akin to non-alcoholic fatty liver disease (NAFLD) marked by accumulation of lipid droplets in hepatocytes, changes in gene expression and activation of inflammatory pathways. Key components of this change could be reproduced by administration of EVPs isolated from tumor explants or cultured cells and were attributed to all three fractions of these isolates, namely exomeres, small exosomes and large exosomes, as distinguished following AF4 separation. Targeting Rab27a in cancer cells attenuated the ability of this material to evoke hepatic toxicity. EVP uptake studies indicated that their main cellular targets are hepatic Kupfer cells (KCs), which were found to upregulate inflammatory cytokines, including TNFa following EVP exposure, in a manner attributable to their apparently altered lipid content, especially the enrichment with palmitic acid (PA) acting upon TLR4 in these cells. TNFa released by KCs, as a result, deregulated CYP pathway in hepatocytes leading to NAFLD-like changes, including formation of intracellular lipid droplets. Targeting Kupfer cells (clodronate), PA synthase (C75) TLR4 receptor (TAK), and TNFa (antibody) attenuated various aspects of the EVP effect on the KC-hepatocyte axis. Finally, these results were found congruent with studies on liver dysfunction in patients with pancreatic cancer without liver metastasis. It is suggested that the metastasis-unrelated impact of cancer EVPs on liver function represents a part of the poorly understood systemic cancer syndrome and a source of poor tolerance to medication in cancer patients, with presently unexplored opportunities to intervene.

This is a very interesting, imaginative, well designed and unconventional study looking beyond the impact of the tumor mass on the constituents of the physical decline in cancer patients. While studies on paraneoplastic syndromes in cancer have been ongoing for quite some time, including cachexia, thrombosis, inflammation and other states, and in some cases with an eye on the role of various EVPs, the liver toxicity remains relatively poorly understood and the present study takes this problem to considerable mechanistic depth. This said, several questions need to be raised with regard to the evidence presented, as well as conclusions and interpretations.

1. The manuscript is somewhat ‘EVP-centric’ in that the authors observe a far greater fatty liver degeneration in tumor bearing mice than upon EVP education and they suggest that non-EVP factors may be involved, but they choose not to study them. This approach makes it difficult to assess how

important are EVPs in the grand scheme of things, and whether they may cooperate with soluble factors in a manner important for NAFLD development.

2. It is very intriguing that in PDAC without liver metastasis the authors detect signs of NAFLD-inducing mechanisms. However, none of the mouse models used in the study are pancreatic cancers and these scenarios are difficult to compare, unless one assumes that NAFLD is an unspecific consequence of any cancer. Is there a relationship between the histological, molecular or clinical features of cancers and their ability to induce NAFLD. What are the boundaries of real life cancer that the mouse models actually reflect?

3. Related to that is the question about the extent of NAFLD across different cancers and non-cancer states, which is presently somewhat unclear. One wonders whether in advanced metastatic cancer liver steatosis is uniquely important, or is a part of multiple system failure, including cachexia and other states (He et al 2014; Chitti et al 2018)? In other words what makes liver changes of particular interest or actionable? Another practical question is whether attenuation of NAFLD in such disseminated cancers (e.g. by targeting TNFa) may still open the widow of opportunity for more meaningful chemotherapy. This is suggested but not examined. Does NAFLD impact anticancer immunity, and does it interfere with treatment with immune checkpoint inibitors, which have become the mainstay in metastatic melanoma, one of the key models used in the present study?

4. As much as one is fascinated by the results and impressed with the depth of the analysis, there are also certain gaps, if not contradictions, in the study of EVP populations. For one, Rab27a targeting is used to demonstrate that without the EVP mechanism cancer cells do not efficiently trigger the NAFLD-like condition. However, not all populations of exosomes depend on Rab27a (Ostrowski et al 2010; Bobrie et al 2012), while the role of this GTPase in exomere release has not been documented. Without the latter information the results of Rab27a silencing on exomere-induced NAFLD cannot be interpreted. This would require some experimental verification and clarification.

5. One remaining question is whether the effects of EVPs on Kupfer cells and hepatocytes are cancer specific? Human blood contains upward of ~1011 EVPs per mL, only a small fraction of which (perhaps <1%) may be cancer-related. The turnover of both endogenous EVPs and therapeutic EVs involves liver uptake and even non-transformed cells produce EVPs containing certain amounts of PA as is clear in the data presented. Why the enormous excess of normal EVPs present in blood does nor cause liver uptake and NAFLD, while cancer EVPs do so? A corollary to this is whether NAFLD an unforeseen long-term consequence of all bolus injections of EVPs, including those currently developed for therapies? Or is there anything specific about EVPs from cancer cells, or do cancer EVP cooperate with other cancer-related factors as the authors seem to suggest (e.g. cytokines). This can be tested by co-treatment with EVPs and culture supernatants.

6. The evidence for the TNFa involvement in EVP-driven NAFLD is highly intriguing, although not unexpected. However, given the existing data, it is difficult to exclude a possibility that TNFa could also be released by cancer cells, and not only from KCs. This could be easily verified.

7. There are also some questions related to the experimental side of the study.

(i) In several experiments the effects of EVPs are compared to untreated controls, PBS or other unspecified controls. This is not ideal, as it does not address the specificity of the EVP sources. Control EVPs (e.g. from normal cells, or blood borne) should be more widely used as controls.

(ii) The vast majority of the experimental analysis is based on two murine cancer cell lines that have been in passage for decades (e.g. B16F10). Since there are no obvious immune components of the process observed, at least as presented, it is unclear why some of the experiments could not have been performed with patient-derived human cancer cells, PDX grafts, organoids, or in transgenic systems that would offer a more faithful, diverse and molecularly defined reflection of cancer biology. At least some of these possibilities could probably be considered.

(iii) Micrometastases in the liver could often be overlooked. Can the authors rule out the effects of micrometastatic disease?

(iv) Among factors that regulate the pathogenesis of NAFLD and NASH are inflammatory cells that could be expected to be recruited by cytokines recorded by the authors in KCs following EVP exposure. Is the influx of inflammatory myeloid cells a part of the EVP effects?

(v) It might be useful to determine how may cancer EVPs are present in the circulation and compare this to the amount being injected during education experiments.

7. Minor concerns:

(i) The manuscript, while well written, is inundated with unnecessary abbreviations (e.g. KC, LD, PCLS, B16F10-Tb and may others). This makes the reading of the paper difficult.

(ii) The nature of controls should be specified in all figures.

(iii) There is a vast literature on EV homing to the liver upon exogenous injection, which may be worth acknowledging beyond authors own work.

Referee #2 (Remarks to the Author):

The view of cancer pathogenesis has expanded from cell-intrinsic to cell-extrinsic regulation, and cancer is now viewed as a systemic disease. Tumors can deregulate the physiology of distant organs without metastasizing to that organ. Little is known about how tumors reprogram systemic physiology and what are the consequences of these systemic effects on the host. The study by Wang et al. provides novel insights into these fundamental biological questions.

This study describes a new mechanism of reprogramming liver metabolism by tumors that do not metastasize to the liver. The authors show that tumor-derived extracellular vesicles and particles (EVPs) reprogram liver metabolism by carrying fatty acids (cargo) to Kupffer cells, which induces the secretion of TNF-alpha. This process of EVP education creates a pro-inflammatory milieu that

suppresses fat metabolism and oxidative phosphorylation in the liver and leads to fatty liver formation. Through genetic studies, the authors demonstrate the function of EVPs in fatty liver formation and their impact on anti-cancer drug metabolism. Complementary to the experimental studies, the authors show that the fatty liver phenotype is also observed in pancreatic cancer patients with tumor-free livers. These novel mechanistic studies reveal a new facet of systemic regulation by tumors and are timely. These studies can have a high clinical impact and can inform treatment decisions. The study is well-controlled with rigor and statistical considerations. A few comments that need to be addressed are listed below.

The clinical data includes patients with a fatty liver at diagnosis who later developed extra-hepatic metastasis. Does fatty liver formation after EVP injection increase the risk of extra-hepatic metastasis in mouse models? If fatty liver is first induced by EVP education, followed by injection of cancer cells via circulation (e.g., via the tail vein), this point can be experimentally tested.

It will be interesting to know how TNF-alpha regulates lipid accumulation in hepatocytes in EVP-injected mice. Is it increased synthesis of lipid droplets or inhibition of lipid catabolism, or both?

Do acute phase proteins (APP) get induced in the hepatocytes during fatty liver formation in EVP-injected mice? APP upregulation could be an early indicator of cachexia. On a related point, is there a visible impact of such liver reprogramming on skeletal muscle or adipose tissue? In other words, is cachexia another systemic effect associated with fatty liver formation?

The authors show that TNF-alpha neutralization in mice reverses lipid droplet accumulation in the liver. Does TNF-blockade reverse the impaired drug metabolism through CYPs? This data could have important treatment implications.

Is the fatty liver phenotype observed in allografts/genetic models of pancreatic cancer? This data would cross-validate the clinical observations.

A more detailed histological staining and quantitation of the fatty liver phenotype (Fig. 1 and Extended data 1) longitudinally in mouse models would clarify the kinetics, extent, and severity of the phenotype.

The fluorescence-based EVP tracking experiment in-vivo is elegant. Can the authors track where the EVP cargo gets taken up besides the liver?

An interesting question is what dictates whether the EVPs will form a pre-metastatic niche (PMN) or generate fatty liver in the liver microenvironment. The authors have mentioned this point in the Discussion section, but a more detailed discussion will clarify this important distinction.

Referee #3 (Remarks to the Author):

The study submitted by Dr. Lyden and colleagues investigated the role of tumor-derived EVPs in the

development of fatty liver and demonstrated its underlying mechanism and the clinical implication by focusing on the drug metabolism capacity. First, the authors used B6F10 and K7M2 lung metastasis models and found gene expression profiles are different in the tumor-free liver of tumor bearing mice compared to the normal liver and fatty liver was induced in tumor-bearing mice. The study further identified that tumor-derived EVP is responsible for fatty liver development. Secreted EVPs were mainly uptaken by Kupffer cells. Also, the study revealed that PDAC patients without liver metastasis developed fatty liver, supporting the findings from mouse experiments. The study also investigated the underlying mechanisms. EVP stimulated Kupffer cells to produce TNFa through TLR4 and this TNFa induced fatty liver. Lastly, the study showed that drug metabolism capacity was decreased by tumor-derived EVPs. These results are very interesting and the experimental approaches are very logic. Especially, the experiment using Rab27a silencing in tumor cells is a good approach. Overall, the study is very interesting. One question is whether decreased drug metabolism by tumor-derived EVPs is associated with fatty liver or whether fatty liver development is necessary for decreasing drug metabolism is unclear. If these are independent, what is the clinical implication of tumor-derived EVP-induced fatty liver?

Specific comments:

1. Figure 1b (and Extended Figure 1e,g). This reviewer agrees that decreased fatty acid metabolism and oxidative phosphorylation could be associated with fatty liver development. However, adipogenesis signature was decreased. Is this in contrast to increased fatty liver? Similarly, in Fig.2d,e, EVP injection decreased adipogenesis signature.

2. Figure 1J showed all pancreatic cancer patients had fatty liver. The text mentioned BMIs are same between cancer patients and control patients. Figure 1J included 4 cancer patients and 5 control patients, but Supplementary Table 5 included 12 controls and 8 PDAC patients. The sample number for fatty liver evaluation should increase to gain a sufficient power, and reassessment of BMI should strongly be recommended. Otherwise, the data are highly biased. Also, BMI could affect fatty liver. For example, control patients with high BMI (e.g. BMI>30) are highly expected having fatty liver.

3. Figure 5j suggested PA in EVPs induced TNFa through TLR4. However, Lancaster et al (PMID: 29681442) reported that TLR4 is not a receptor for palmitate. How can the authors explain it?

4. The authors tested several drugs and showed drug metabolism for those drugs were decreased. What is the metabolism of anti-cancer chemo drugs in hepatocytes affected by tumor-derived EVPs? May these drugs cause more toxicity to host or cancer?

5. The authors found tumor-derived EVPs induced fatty liver and decreased drug metabolism. Is this fatty liver associated with decreased drug metabolism or tumor-derived EVPs can decrease drug metabolism independently of fatty liver?

Author Rebuttals to Initial Comments:

Referees' comments:

Referee #1 (Remarks to the Author):

The study by Wang explores the systemic effects of cancer-derived extracellular vesicles and particles (EVPs), especially as inducers of fatty liver disease. This represents an aspect of systemic cancer progression unrelated to liver metastasis. The authors noted that cancer-associated liver disfunction is and important but poorly understood paraneoplastic pathology that can be recapitulated in models of transplantable murine cancers, such as B16F10 melanoma, K7M2 osteosarcoma and mammary cancers (67NR and subline of 4T1). While these tumors did not form overt liver metastases, they remotely triggered a condition akin to non-alcoholic fatty liver disease (NAFLD) marked by accumulation of lipid droplets in hepatocytes, changes in gene expression and activation of inflammatory pathways. Key components of this change could be reproduced by administration of EVPs isolated from tumor explants or cultured cells and were attributed to all three fractions of these isolates, namely exomeres, small exosomes and large exosomes, as distinguished following AF4 separation. Targeting Rab27a in cancer cells attenuated the ability of this material to evoke hepatic toxicity. EVP uptake studies indicated that their main cellular targets are hepatic Kupfer cells (KCs), which were found to upregulate inflammatory cytokines, including TNFa following EVP exposure, in a manner attributable to their apparently altered lipid content, especially the enrichment with palmitic acid (PA) acting upon TLR4 in these cells. TNFa released by KCs, as a result, deregulated CYP pathway in hepatocytes leading to NAFLD-like changes, including formation of intracellular lipid droplets. Targeting Kupfer cells (clodronate), PA synthase (C75) TLR4 receptor (TAK), and TNFa (antibody) attenuated various aspects of the EVP effect on the KC-hepatocyte axis. Finally, these results were found congruent with studies on liver dysfunction in patients with pancreatic cancer without liver metastasis. It is suggested that the metastasis-unrelated impact of cancer EVPs on liver function represents a part of the poorly understood systemic cancer syndrome and a source of poor tolerance to medication in cancer patients, with presently unexplored opportunities to intervene.

This is a very interesting, imaginative, well designed and unconventional study looking beyond the impact of the tumor mass on the constituents of the physical decline in cancer patients. While studies on paraneoplastic syndromes in cancer have been ongoing for quite some time, including cachexia, thrombosis, inflammation and other states, and in some cases with an eye on the role of various EVPs, the liver toxicity remains relatively poorly understood and the present study takes this problem to considerable mechanistic depth. This said, several questions need to be raised with regard to the evidence presented, as well as conclusions and interpretations.

Authors: We greatly appreciate the reviewer's positive assessment of our work. In response to the reviewer's thoughtful comments, we have performed numerous additional experiments, aiming to address all of the reviewer's concerns.

1. The manuscript is somewhat 'EVP-centric' in that the authors observe a far greater fatty liver degeneration in tumor bearing mice than upon EVP education and they suggest that non-EVP factors may be involved, but they choose not to study them. This approach makes it difficult to assess how important are EVPs in the grand scheme of things, and whether they may cooperate with soluble factors in a manner important for NAFLD development.

Authors: We thank the reviewer for this comment. To determine if soluble factors secreted by tumor cells could contribute to fatty liver generation, we intra-peritoneally injected mice with control media or EVP-depleted conditioned media (CM) from B16F10 or K7M2 cells, which is concentrated from a volume equivalent to that required for the isolation of 10 μg of EVPs, every other day for 4 weeks, the same procedure utilized for EVP education. Briefly, we first performed the ultracentrifugation (at 100,000g for 70 min) of the CM of cultured cancer cells to separate the EVPs (the pellet) and obtain the EVP-depleted CM (media supernatant). Then, the EVP-depleted CM was concentrated using Amicon Ultra-15 centrifugal filters with 10 KDa cutoff spun at 4,000g at 4 °C. Blank media (DMEM supplemented with 10% EVP-depleted FBS and 1× penicillin/streptomycin) was also concentrated and used as control media. In general, 5 ml of cell culture CM yields approximately 10 μg of EVPs. The same volume of EVP-depleted CM was further concentrated to a volume of 200 μl and used for each injection. Importantly, administration of tumor cell-derived EVP-depleted CM every other day for 4 weeks did not generate fatty liver (**Response to Reviewers Figure 1a**,**b**, also included in the manuscript as **Extended Data Figure 4o**), suggesting that non-EVP tumor secreted factors are not sufficient/responsible for fatty liver formation.

Furthermore, to determine if EVP-depleted CM could enhance EVP-induced fatty liver generation, we intra-peritoneally injected 200 μl of concentrated EVP-depleted CM together with intravenous injection of 10 μg of B16F10 cell line-derived EVPs (B16F10-CL-EVPs), every other day for 4 weeks. However, in comparison with EVP-education alone, administration of EVP-depleted CM did not enhance EVP-education-induced fatty liver formation (**Response to Reviewers Figure 1c**, also included in the manuscript as **Extended Data Figure 4p**), indicating that non-EVP tumor secreted factors are not necessary for fatty liver generation and tumor EVPs are sufficient to promote the accumulation of lipids in the liver.

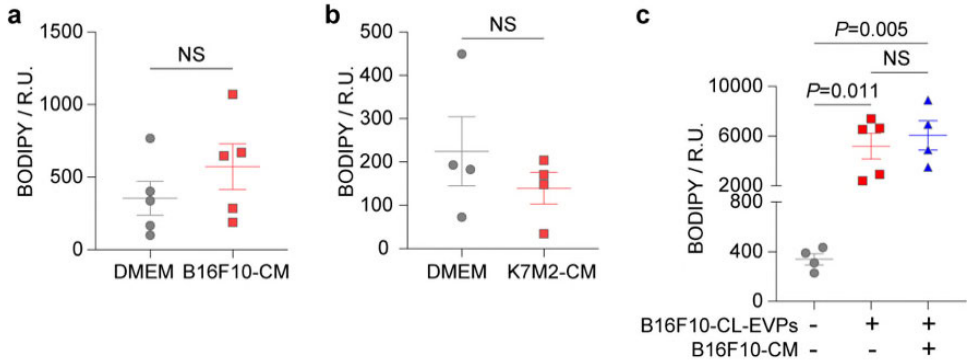

Response to reviewers Figure 1. EVP-depleted conditioned media (CM) from cultured cancer cells cannot induce fatty liver generation. a,**b**, Statistical analysis of BODIPY staining of the livers from B16F10-CM (**a**) and K7M2-CM (**b**) educated mice, compared to DMEM-educated mice. n=5 mice per group for B16F10-CM model and n=4 mice per group for K7M2-CM model. **c**, Statistical analysis of BODIPY staining of the livers from PBS-educated and B16F10-CL-EVP-educated mice, in the absence or presence of B16F10-CM co-education. n=4 mice educated by PBS, n=5 mice educated by B16F10-CL-EVPs alone, and n=4 mice educated by B16F10-CL-EVPs together with B16F10-CM. *P* values were determined by the two-tailed, unpaired Student's *t*-test (**a**,**b**), or one-way ANOVA with post hoc Tukey's test for (**c**). NS, not significant. Data are represented as mean ± s.e.m.

Moreover, we showed that *Rab27a* silencing reduced EVP secretion from the tumor cells and suppressed tumor-induced lipid droplet accumulation in the liver (**Response to Reviewer Figure 2**, from manuscript

Extended Data Figure 5c,d, and Figure **3c,d**). This result further supports our findings that tumor EVPs, but not non-EVP soluble factors, are responsible for tumor-induced fatty liver generation, since we and others have reported that *Rab27a* silencing has no or very limited effect on the secretion of non-EVP soluble factors from tumor cells (Bobrie et al., 2012; Ostrowski et al., 2010; Peinado et al., 2012).

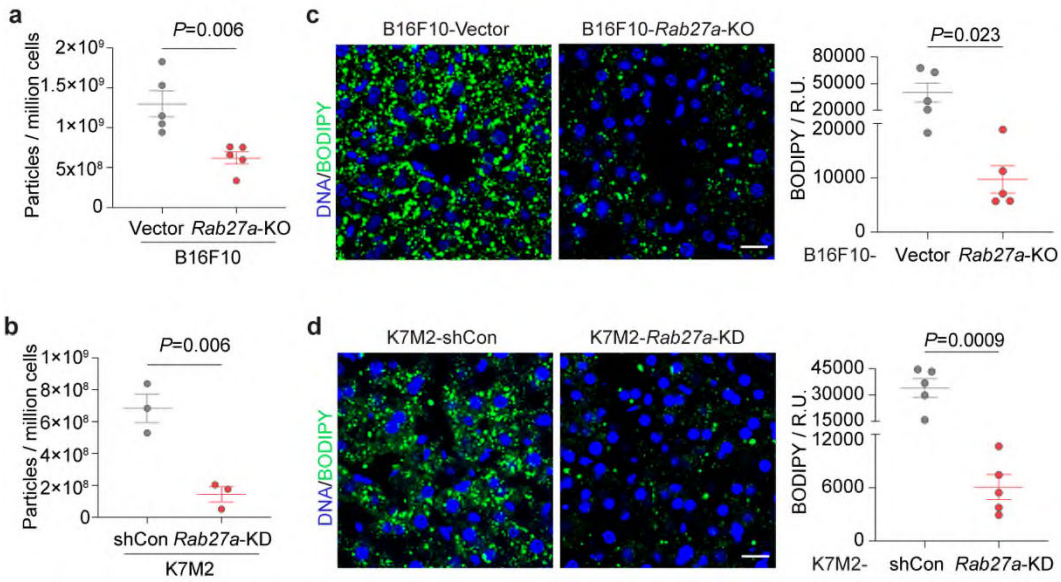

Response to reviewers Figure 2. *Rab27a* silencing reduced EVP secretion from the tumor cells and suppressed tumor-induced fatty liver formation. a, Nanoparticle tracking analysis (NTA) of the numbers of EVPs secreted by B16F10-control (Vector) or B16F10-*Rab27a*-KO cells. n=5 independent experiments per group. **b** NTA of the numbers of EVPs secreted by K7M2-control (shCon) or K7M2-*Rab27a*-KD cells. n=3 independent experiments per group. **c**,**d**, Representative images (left) and associated statistical analysis (right) of BODIPY staining of the livers from B16F10-*Rab27a*-KO (**c**) and K7M2-*Rab27a*-KD (**d**) tumor bearing mice, and their respective controls. n=5 mice per group. *P* values were determined by the two-tailed, unpaired Student's *t*-test. Data are represented as mean ± s.e.m.

We speculate that the greater fatty liver generation in tumor-bearing mice is due to the fact that tumor cells constantly secrete a large number of EVPs into the circulation (data shown below), compared to the 10 µg of EVPs injected every other day during our education experiments.

2. It is very intriguing that in PDAC without liver metastasis the authors detect signs of NAFLD-inducing mechanisms. However, none of the mouse models used in the study are pancreatic cancers and these scenarios are difficult to compare, unless one assumes that NAFLD is an unspecific consequence of any cancer. Is there a relationship between the histological, molecular or clinical features of cancers and their ability to induce NAFLD. What are the boundaries of real life cancer that the mouse models actually reflect?

Authors: We thank the reviewer for these insightful comments. To address the reviewer's comments, we performed several experiments employing genetically engineered mouse models (GEMMs) of pancreatic ductal adenocarcinoma (PDAC) and melanoma, patient-derived primary melanoma cell lines, and osteosarcoma patient-derived xenografts. We also further strengthened our analysis of patient specimens.

First, we studied tamoxifen-inducible KPC mice (*Kras*^{tm4Tyj} *Trp53*^{tm1Brn} Tg[Pdx1-cre/Esr1*]#Dam/J), a PDAC GEMM, generated as previously described (Maddipati and Stanger, 2015). Briefly, *Trp53* excision was induced in pups via lactation upon administration of tamoxifen (6 mg/mouse) via oral gavage to the dam. Mice carrying the *Kras*^{G12D} mutation in one allele (*Kras*$^{WT/G12D}$) developed pancreatic intraepithelial neoplasia (PanIN) lesions at 8-10 weeks of age, which progressed into local PDAC at 10-14 weeks and invasive PDAC at 15-18 weeks, associated with distant metastasis to several sites including lymph nodes, liver, lungs, diaphragm, and spleen. Since liver metastasis can always be detected in 20-week-old tumor-bearing mice, the liver of 14-week-old tumor-bearing mice, prior to tumor cell seeding of the liver, represents the pre-metastatic niche (PMN) (**Response to reviewers Figure 3a**, also included in the manuscript as **Extended Data Fig. 2j**). However, lipid droplet accumulation was not detected in pre-metastatic livers of 14-week-old tumor-bearing KPC mice (**Response to reviewers Figure 3b**, also included in the manuscript as **Extended Data Fig. 2k**). We speculate that genetic murine model of PDAC induces PMN formation, which precludes the generation of fatty liver. This finding supports our hypothesis that tumors with extrahepatic metastatic tropism, but not those with liver tropism, induce fatty liver generation, as we have shown in multiple non-liver metastatic cancer models, including melanoma, breast cancer and osteosarcoma.

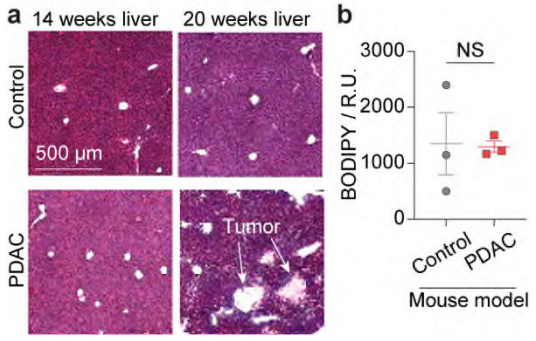

Response to reviewers Figure 3. Fatty liver is not induced in liver-metastatic KPC PDAC GEMM. a, Representative H&E staining images of the livers from KPC mice. Liver metastasis was observed in 20-week, but not 14-week tumor bearing mice. Scale bar, 500 μm. **b**, Statistical analysis of BODIPY staining of the livers from 14-week PDAC tumor-bearing mice, compared to non-PDAC mouse controls. n=3 mice per group. *P* values were determined by the two-tailed, unpaired Student's *t*-test. Data are represented as mean ± s.e.m.

Furthermore, we employed a genetic murine model of spontaneous melanoma, which does not develop liver metastasis (Burd et al., 2014). In brief, C57BL/6 *TN* mice carrying a Cre-inducible *Nras*^{Q61R} oncogene, were treated topically with 20mM 4-hydroxytamoxifen (4-OHT) on postnatal days 1 and 2 to activate melanocyte-specific CRE recombination driven by the Tyr-CRE-ER(T2) transgene. On postnatal day 3, pups received 1.5 SED (standard erythemal dose) of solar radiation. Animals were monitored for spontaneous tumor formation and euthanized upon reaching exclusion criteria (tumor length ≥ 1.6cm or ulceration ≥ 2mm). Non-tumor bearing control mice carried the *Nras*^{Q61R}, *p16*$^{fl/fl}$ and Tyr-CRE-ER(T2) alleles but were not treated to induce CRE activity or tumor formation. Functionally null *Mc1r* increased melanoma susceptibility (**Response to reviewers Figure 4a**, also included in the manuscript as **Extended Data Figure 1a**). BODIPY staining revealed the formation of fatty liver in these tumor-bearing mice, compared to no tumor controls (**Response to reviewers Figure 4c**, also included in the manuscript as **Extended Data Figure 2i**), demonstrating that our observations are not limited to experimental models of cancer but can be

reproduced in GEMM of melanoma. These observations further support our hypothesis that tumors without liver metastasis induce fatty liver generation.

Liver biopsies/specimens from patients with melanoma or osteosarcoma are not available since it cannot be ethically justified as part of standard of care. Thus, to validate the clinical relevance of melanoma- and osteosarcoma-induced fatty liver, we investigated whether human cell line or patient-derived xenografts (PDXs) generated from these cancers could also induce fatty liver formation. We studied the patient-derived melanoma SK-MEL-192 cell line, and primary osteosarcoma PDXs generated from 7 patients who underwent tumor removal surgery at Memorial Sloan Kettering Cancer Center (**Response to reviewers Figure 4a**, also included in the manuscript as **Extended Data Figure 1a**; osteosarcoma patient information was described in the manuscript as **Supplementary Table 5a**). In brief, SK-MEL-192 cells and osteosarcoma PDXs were subcutaneously implanted into nude and NSG mice, respectively. Three weeks later, the SK-MEL-192 tumor-bearing mice were confirmed to be free of liver metastasis via H&E staining. For osteosarcoma PDXs, no liver metastasis was detected by magnetic resonance imaging (MRI), while lung metastasis occurred in the osteosarcoma PDX model 4-8 weeks post-tumor implantation (**Response to reviewers Figure 4b**, also included in the manuscript as **Extended Data Figure 1b,d**). Strikingly, fatty liver was detected in both models (**Response to reviewers Figure 4c**, also included in the manuscript as **Extended Data Figure 2i**). Thus, our finding of fatty liver induction by tumors without liver metastatic tropism is recapitulated in patient-relevant models, demonstrating its relevance to the biology of human melanoma and osteosarcoma.

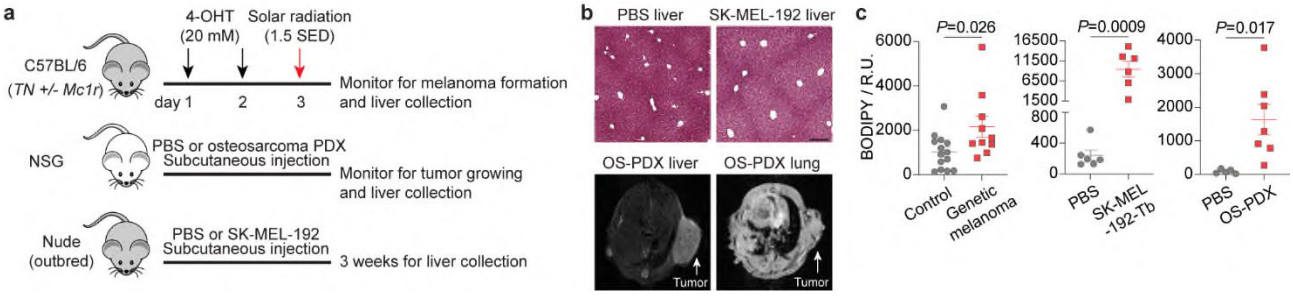

Response to reviewers Figure 4. Fatty liver can be induced in multiple tumor models without liver metastasis. a, Schematic representation of melanoma GEMM, osteosarcoma patient-derived xenograft (PDX) and human melanoma cell (SK-MEL-192) tumor-bearing models assessed in this study. Primary osteosarcoma PDX (OS-PDX) models were generated by transplanting the freshly excised surgical tumor specimens from osteosarcoma patients into female NOD/SCID/IL2Rγ^{null} (NSG) mice (OS-PDX). PDX tumor growth became evident during the first 1–2 weeks after engrafting and became excisable for harvesting within a total of 4–8 weeks. NSG mice injected with PBS were used as controls. SK-MEL-192 cells were subcutaneously injected into nude (outbred) mice. Mice injected with PBS served as controls. Three weeks later, livers were collected for downstream analysis. **b**, Representative H&E staining images and Magnetic Resonance Imaging (MRI) images showing liver metastasis was undetectable in SK-MEL-192 and OS-PDX tumor-bearing mice, but lung metastasis was detected in OS-PDX tumor-bearing mice. Scale bar, 200 μm. **c**, Statistical analysis of BODIPY staining of the livers from melanoma GEMM, human melanoma SK-MEL-192-Tb mice and human OS-PDX tumor-bearing mice, and their respective controls. n=14 control and n=10 tumor-bearing mice for genetic melanoma model; n=6 mice per group for SK-MEL-192 model; n=5 control and n=7 tumor-bearing mice for OS-PDX model. *P* values were determined by the two-tailed, unpaired Student's *t*-test. Data are represented as mean ± s.e.m. Tb, tumor-bearing.

Moreover, to expand the number of patients in this study, we accrued livers from 10 additional subjects, 7 of which were PDAC patients without liver metastasis and 3 control subjects with benign lesions. This cohort of PDAC patients is a very specific subset, which accounts for 10-30% of total PDAC patients, as they only developed extrahepatic metastasis. Importantly, fatty liver generation was confirmed in PDAC patients without liver metastasis but not controls (**Response to reviewers Figure 5**, also included in the manuscript as **Figure 1j**). These data demonstrate that cancer-induced fatty liver occurs only in cancer patients who do not develop hepatic metastasis.

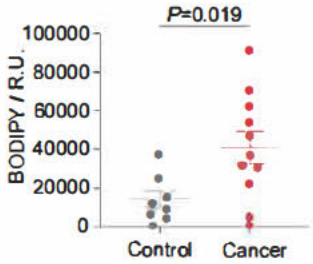

Response to reviewers Figure 5. Fatty liver can be induced in PDAC patients without liver metastasis. Statistical analysis of BODIPY staining of the livers from pancreatic cancer patients and control subjects with benign lesions. n=11 pancreatic cancer patients and n=8 control subjects. *P* values were determined by the two-tailed, unpaired Student's *t*-test. Data are represented as mean ± s.e.m.

3.1. Related to that is the question about the extent of NAFLD across different cancers and non-cancer states, which is presently somewhat unclear. One wonders whether in advanced metastatic cancer liver steatosis is uniquely important, or is a part of multiple system failure, including cachexia and other states (He et al 2014; Chitti et al 2018)?

Redacted text

Redacted text and figure

3.2 In other words what makes liver changes of particular interest or actionable? Another practical question is whether attenuation of NAFLD in such disseminated cancers (e.g. by targeting TNFa) may still open the widow of opportunity for more meaningful chemotherapy. This is suggested but not examined.

Authors: Liver is the central metabolic organ and required for host systemic metabolic homeostasis as well as drug metabolism. Thus, we hypothesized that liver function can be critically dysregulated upon fatty liver induction by growing tumors and one outcome could be impaired drug metabolism. In cancer patients in particular, fatty liver may lead to increased adverse toxicity associated with standard chemotherapy, rendering it critical and promising for therapeutic targeting.

To address the reviewer's comment, we first sought to determine if fatty liver induced by tumor-derived EVPs can affect chemotherapy-induced toxicity *in vivo*. We educated mice with B16F10- or K7M2-CL-EVPs (PBS or primary osteoblast-derived EVPs were used as controls, respectively) to induce fatty liver, then treated these mice with chemotherapeutic drugs used in patients, such as dacarbazine (used in melanoma) and doxorubicin (used in osteosarcoma) (**Response to reviewers Figure 7a**, also included in the manuscript as **Extended Data Figure 10c**). These drugs can be metabolized by cytochrome P450 enzymes (Bagdasaryan et al., 2022; Lewis et al., 2007; Reid et al., 1999), whose functions are impaired in fatty livers as shown in this work. Importantly, tumor EVP-induced fatty liver generation correlated with increased chemotoxicity, as shown by enhanced dacarbazine-induced bone marrow depression (including reduced red blood cells, reticulocytes and hemoglobin levels as shown in **Response to reviewers Figure 7b**, also

included in the manuscript as **Figure 6g**) and doxorubicin-induced cardiotoxicity (including reduced left ventricular ejection fraction and fractional shortening as shown in **Response to reviewers 7c,d**, also included in the manuscript as **Figure 6h** and **Extended Data Figure 10e**). These results suggest that tumor EVP-induced fatty liver correlates with and likely promotes the adverse side effects of standard chemotherapies normally metabolized in the liver.

In the manuscript, we showed that TNFα blockade reduced fatty liver generation in both tumor-bearing mice and EVPs educated mice (data in the manuscript **Figure 5e,f**, which are shown here in **Response to reviewers 7e,f**). Therefore, TNFα blockade, through hindering fatty liver formation, could indeed limit chemotherapy-associated systemic toxicity, creating a window for improving the efficacy of chemotherapy, which is of critical importance for cancer patient treatment and outcomes.

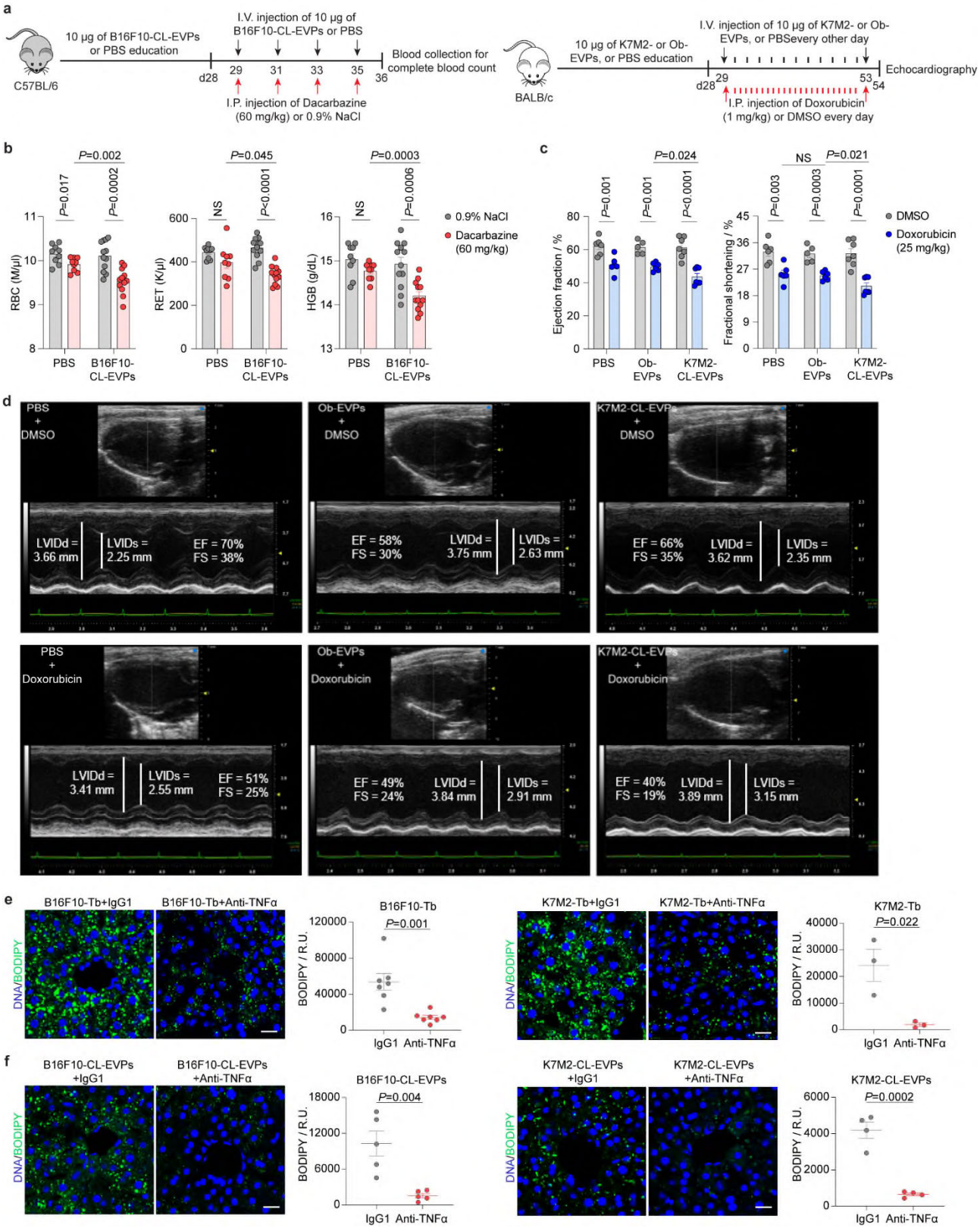

Response to reviewers Figure 7. Tumor EVP-induced fatty liver enhances the systemic toxicity of chemotherapy. a, Schematic illustration of the procedure for performing chemotoxicity analysis using EVP-educated mice. For B16F10-CL-EVP education model (left), C57BL/6 mice were intra-venously

injected with PBS or 10 μg of B16F10-CL-EVPs every other day for 4 weeks, then intra-peritoneally injected with dacarbazine (60 mg/kg) or 0.9% NaCl together with intra-venous injection of PBS or 10 μg of B16F10-CL-EVPs every other day, 4 times. Blood was then collected for complete blood count (CBC). For the K7M2-CL-EVP education model (right), BALB/c mice were intra-venously injected with PBS or 10 μg of osteoblast-EVPs (Ob-EVPs) or K7M2-CL-EVPs every other day for 4 weeks, then intra-peritoneally injected with doxorubicin (1 mg/kg) or DMSO every 24 h together with intra-venous injection of PBS or 10 μg of osteoblast-EVPs or K7M2-CL-EVPs every other day for 25 days. The cumulative dose of doxorubicin was 25 mg/kg, and mice were then subjected to echocardiography. **b**, Statistical analysis of the features of red blood cell (RBC), reticulocyte (RET) and hemoglobin (HGB) in the PBS- or B16F10-CL-EVP-educated mice after treatment of Dacarbazine (60 mg/kg) or 0.9% NaCl. n=9 mice for PBS groups and n=12 for B16F10-CL-EVP groups. **c**, Statistical analysis of the ejection fraction and ejection shortening (M-mode) in the PBS-, or osteoblast-EVP-, or K7M2-CL-EVP-educated mice after treatment with Doxorubicin (cumulative dose of 25 mg/kg) or DMSO. n=6 mice for PBS groups and n=7 mice for K7M2-CL-EVP groups. n=5 and n=6 for DMSO and Doxorubicin treated osteoblast-EVPs educated mice, respectively. **d**, Representative M-mode images of echocardiography for the PBS- or osteoblast-EVP- or K7M2-CL-EVP-educated mice after treatment of DMSO or doxorubicin (cumulative dose of 25 mg/kg) as described in (**a**,**c**). LVIDd, left ventricular internal dimension at end diastole. LVIDs, left ventricular internal dimension at end systole. EF, ejection fraction. FS, fractional shortening. **e**,**f**, Representative images (left) and statistical analysis (right) of BODIPY staining of the livers from B16F10- and K7M2-Tb mice (**e**), and B16F10-CL-EVP- and K7M2-CL-EVP-educated mice (**f**), treated with anti-TNFα antibody or IgG1 isotype control. For B16F10-Tb model, n=7 mice per group. For K7M2-Tb model, n=3 mice per group. For B16F10-CL-EVP education model, n=5 mice per group. For K7M2-CL-EVP education model, n=4 mice per group. *P* values were determined by multiple unpaired *t*-test and two-tailed, unpaired Student's *t*-test (**b**,**c**), or two-tailed, unpaired Student's *t*-test (**e**,**f**). NS, not significant. Data are represented as mean ± s.e.m. An error was made for the statistical test used in (**b**,**c**). The correct test should have been the two-way ANOVA with Fisher's LSD test, and this correction was included in the second revision.

3.3 Does NAFLD impact anticancer immunity, and does it interfere with treatment with immune checkpoint inibitors, which have become the mainstay in metastatic melanoma, one of the key models used in the present study?

Redacted text

Redacted text and figure

4. As much as one is fascinated by the results and impressed with the depth of the analysis, there are also certain gaps, if not contradictions, in the study of EVP populations. For one, Rab27a targeting is used to demonstrate that without the EVP mechanism cancer cells do not efficiently trigger the NAFLD-like condition. However, not all populations of exosomes depend on Rab27a (Ostrowski et al 2010; Bobrie et al 2012), while the role of this GTPase in exomere release has not been documented. Without the latter information the results of Rab27a silencing on exomere-induced NAFLD cannot be interpreted. This would require some experimental verification and clarification.

Authors: In the original manuscript, we showed that *Rab27a* silencing reduced, but did not completely block EVP secretion (Response to reviewers Figure 9a,b, data shown in the manuscript as Extended Data Figure 5c,d). Furthermore, *Rab27a* silencing dramatically reduced, but did not fully abolish fatty liver formation, as the liver BODIPY staining of *Rab27a*-KO/KD tumor-bearing mice was still much higher (~30 folds) than that of the PBS-injected non-tumor control mice. To improve the clarity of data presentation, we re-graphed the data to render the y-axis easier to interpret (Response to reviewer Figure 9c-f, data shown in the manuscript as Figure 1g,h and Figure 3c,d). Furthermore, to investigate whether *Rab27a*

silencing would interfere with exomere secretion, we performed asymmetric flow field-flow fractionation (AF4) (Zhang et al., 2018; Zhang and Lyden, 2019) on the EVPs isolated from B16F10-Vector control and B16F10-*Rab27a*-KO cells. Remarkably, the secretion of all 3 subpopulations, including exomeres, Exo-S (small exosomes, to a less extent) and Exo-L (large exosomes, to the least extent) were reduced by *Rab27a* silencing (**Response to reviewers Figure 9g**, also included in the manuscript as **Extended Data Figure 5p**). Therefore, these data demonstrate that the production of all EVP subsets is affected partially to different extents by *Rab27a* silencing in B16F10, explaining why *Rab27a* KO led to decrease but not complete abolishment of fatty liver formation.

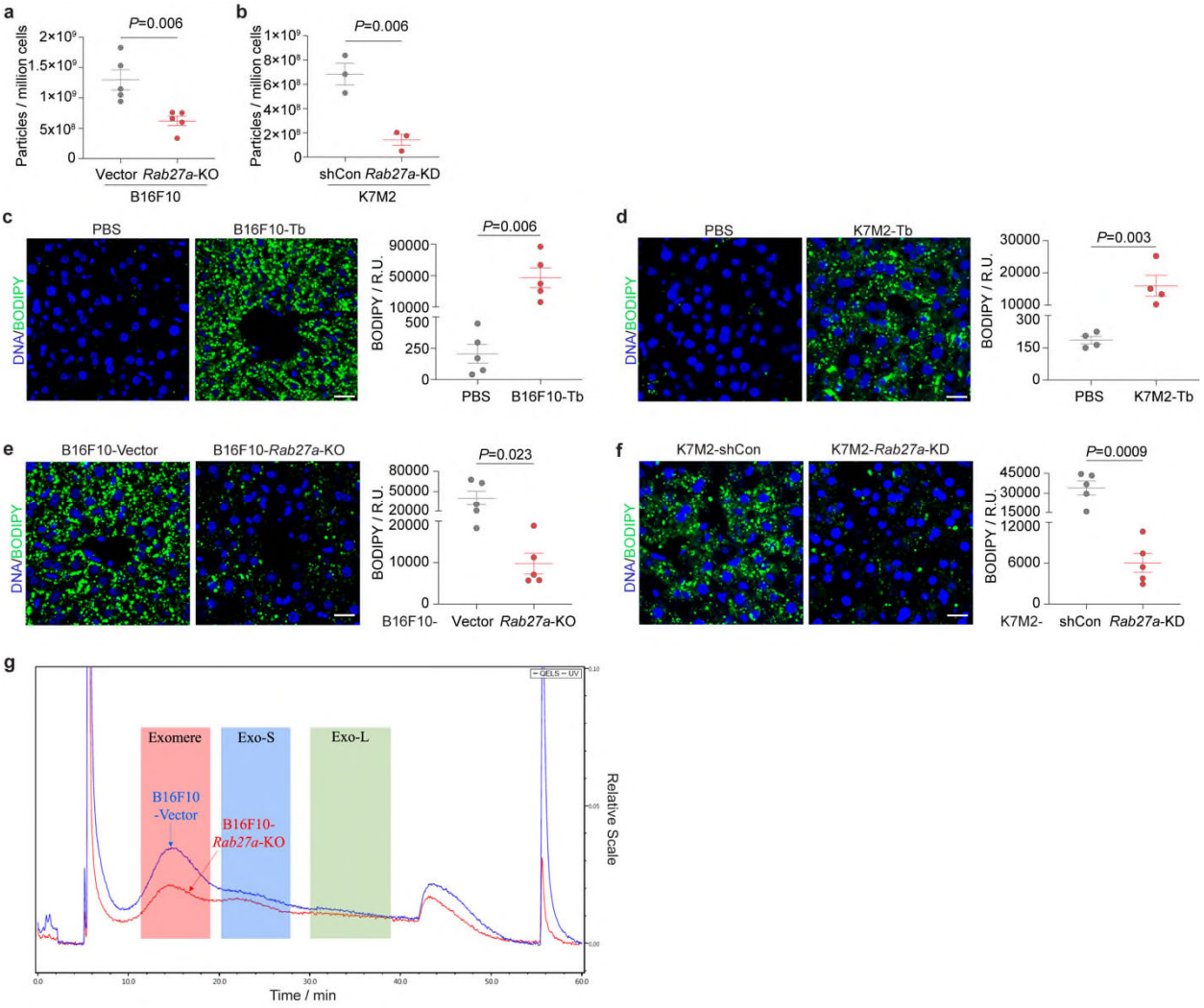

Response to reviewers Figure 9. Ablation of *Rab27a* expression suppressed secretion of all EVP subpopulations from cancer cells. a, NTA of the numbers of EVPs secreted by B16F10-control (Vector) or B16F10-*Rab27a*-KO cells. n=5 independent experiments per group. **b** NTA of the numbers of EVPs secreted by K7M2-control (shCon) or K7M2-*Rab27a*-KD cells. n=3 independent experiments per group. **c**,**d**, Representative images (left) and associated statistical analysis (right) of BODIPY staining of the livers from B16F10-Tb (**c**) and K7M2-Tb (**d**) mice, and their respective PBS-injected controls. n=5 B16F10-Tb mice and controls; n=4 K7M2-Tb mice and controls. **e**,**f**, Representative images (left) and associated statistical analysis (right) of BODIPY staining of the livers from B16F10-*Rab27a*-KO (**e**) and K7M2-*Rab27a*-KD (**f**) tumor bearing mice, and their respective controls. n=5 mice per group. **g,** EVPs isolated from equal numbers of B16F10-Vector control and B16F10-Rab27a-KO cells were resolved via AF4 as previously

described (Zhang *et al.*, 2018; Zhang and Lyden, 2019). Shown are real time measurement of UV on a relative scale (right axis), indicating the abundance of fractionated particles. Shaded areas mark the elution time periods for exomeres (red), Exo-S (blue) and Exo-L (green), respectively. Clearly, as reflected by the UV signal, the production of exomeres, Exo-S (to a less extent) and Exo-L (to the least extent) were reduced in the B16F10-Rab27a-KO cells compared to the B16F10-Vector control cells. *P* values were determined by the two-tailed unpaired *t*-test. Data are represented as mean ± s.e.m.

5. One remaining question is whether the effects of EVPs on Kupfer cells and hepatocytes are cancer specific? Human blood contains upward of ~1011 EVPs per mL, only a small fraction of which (perhaps <1%) may be cancer-related. The turnover of both endogenous EVPs and therapeutic EVs involves liver uptake and even non-transformed cells produce EVPs containing certain amounts of PA as is clear in the data presented. Why the enormous excess of normal EVPs present in blood does nor cause liver uptake and NAFLD, while cancer EVPs do so? A corollary to this is whether NAFLD an unforeseen long-term consequence of all bolus injections of EVPs, including those currently developed for therapies? Or is there anything specific about EVPs from cancer cells, or do cancer EVP cooperate with other cancer-related factors as the authors seem to suggest (e.g. cytokines). This can be tested by co-treatment with EVPs and culture supernatants.

Authors: We thank the reviewer for these thoughtful comments. By performing mass spectrometry-based unbiased proteomics and bioinformatic analysis of a large dataset of tumor tissue- and plasma-derived EVPs, we have previously estimated that tumor-derived EVPs account for ~50% of the total EVPs in the circulation of cancer patients (Hoshino et al., 2020). In support of our findings, using immunoaffinity-based isolation of melanoma cell-derived exosomes, another group found that on average, ~45% of EVPs circulating in the plasma of melanoma patients were tumor-derived (Sharma et al., 2018). Therefore, a large portion of circulating EVPs is indeed tumor-derived.

To address whether the effects of EVPs on Kupfer cells and hepatocytes are cancer specific, we examined whether EVPs derived from normal cells, such as primary osteoblast-derived EVPs (osteoblast-EVPs, short for Ob-EVPs), were also uptaken in the liver. We found that indeed Ob-EVPs were uptaken in the liver to the same extent as tumor-derived EVPs (**Response to reviewers Figure 10a**, also included in the manuscript as **Extended Data Figure 9g**). However, these normal EVPs, including Ob-EVPs, skin tissue explant-derived EVPs (skin-TE-EVPs) and bone tissue explant-derived EVPs (bone-TE-EVPs), could neither induce *Tnf* expression in Kupffer cells nor promote fatty liver generation *ex vivo* in precision-cut liver slices or *in vivo* in mice educated with these EVPs for 4 weeks (**Response to reviewers Figure 10 b-d**, also included in the manuscript as **Extended Data Figure 9 e**,**f**,**h**). In contrast, EVPs from tumor cell lines and tumor tissue explants of both B16F10 and K7M2 models were all able to induce fatty liver generation *in vivo* in educated mice (data shown in the manuscript **Figure 2j**,**k** and **3a**,**b**) and *ex vivo* in the precision-cut liver slices (**Response to reviewers Figure 10c,d**, also included in the manuscript as **Extended Data Figure 9f**,**h**). These data suggest that the functional effects of tumor EVPs in the liver are due to the specific cargo/content of tumor-derived EVPs, rather than specific/restricted liver uptake of these EVPs. This is supported by our previous publication demonstrating, by using unbiased proteomics MS analyses, that the EVP cargo significantly differs between cancer and normal tissues/cells (Hoshino *et al.*, 2020). Thus, we do not expect that non-tumor, normal tissue-derived EVPs employed for therapeutic purposes would promote fatty liver generation and/or negatively impact liver function.

Moreover, we showed in this work that, although palmitic acid (PA) can be detected in EVPs derived from normal tissues/cells, the content of PA is ~2 fold higher in the EVPs derived from tumor tissues/cells (manuscript **Figure 5g,h** and **Extended Data Figure 9a,b**). Other saturated fatty acids, such as stearic acid,

are also highly represented in the tumor EVPs (manuscript **Figure 5g,h** and **Extended Data Figure 9a,b**). Importantly, functional studies including inhibiting PA biogenesis in donor cells and its packaging into tumor-EVPs and blocking its downstream effector in recipient cells (i.e., Kupffer cells) showed that tumor-EVP-packaged PA is critical for inducing fatty liver formation. These findings indicate that fatty liver is not an unforeseen consequence of treatment with any EVPs, but a specific effect of tumor-EVPs due to their distinct cargo.

To address the potential contribution of other tumor-secreted factors to fatty liver formation, following the reviewer's suggestion, we educated mice with EVP-depleted CM together with B16F10-CL-EVPs for 4 weeks. Importantly, CM education was not sufficient to induce fatty liver formation, nor could it enhance EVP-induced fatty liver generation (**Response to reviewers Figure 1a,c**), indicating that tumor EVPs are necessary and sufficient to functionally promote fatty liver generation.

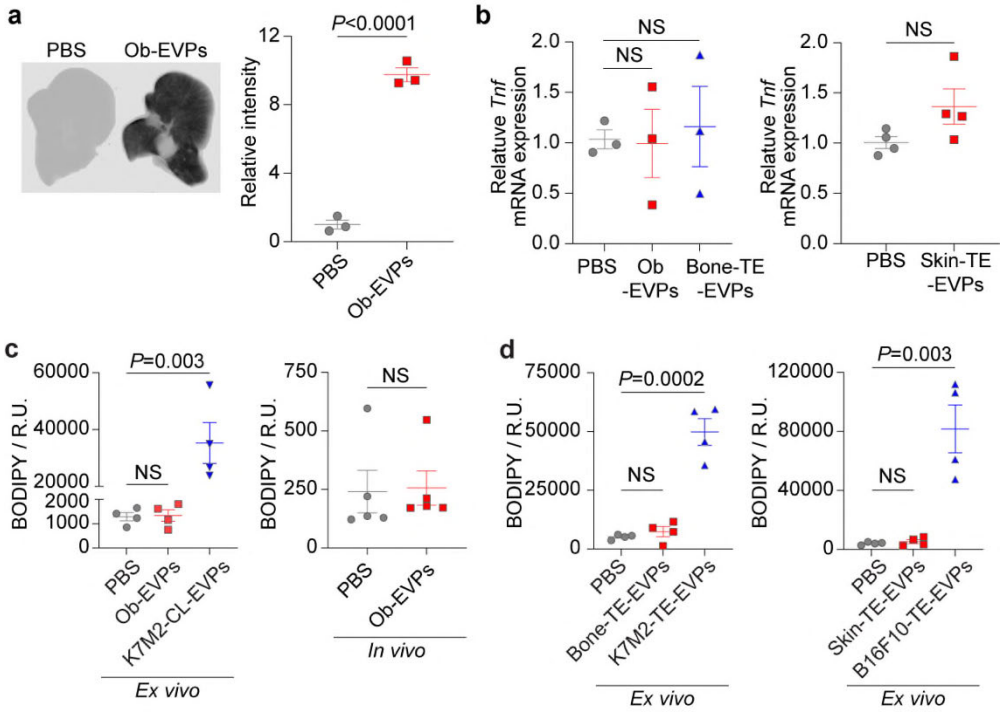

Response to reviewers Figure 10. EVPs derived from normal tissues and cells do not induce fatty liver formation. a, Representative LI-COR Odyssey images (left) and associated statistical analysis of signal intensity (right) of the livers from mice 24 h post intravenously injection of 10 μg of CellVue NIR815 labeled Ob-EVPs and mock PBS-injected control. n=3 mice per group. **b**, qRT-PCR analysis of *Tnf* expression in the KCs isolated from naïve BALB/c mice (left) or C57BL/6 mice (right) and treated with control PBS, or 10 μg/ml of Ob-EVPs and bone-TE-EVPs (left), or 10 μg/ml of skin-TE-EVPs (right) *in vitro* for 4 h. n=3 independent experiments per group for treatment with Ob-EVPs, bone-TE-EVPs, or PBS. n=4 independent experiments for treatment with skin-TE-EVPs or PBS. **c**, Statistical analysis of BODIPY staining of the precision-cut liver slices treated with 10 μg/ml of Ob-EVPs or K7M2-CL-EVPs *ex vivo* for 48 h, or the livers educated by Ob-EVPs in vivo for 4 weeks, compared to PBS-treated or PBS-educated controls, respectively. n=4 mice per group for *ex vivo* EVP treatment and n=5 mice per group for *in vivo* EVP education. **d**, Statistical analysis of BODIPY staining of the precision-cut liver slices treated with control PBS, 10 μg/ml of bone-TE-EVPs or K7M2-TE-EVPs (left), skin-TE-EVPs or B16F10-TE-EVPs (right) *ex vivo* for 48 h. n=4 mice per group. *P* values were determined by the two-tailed, unpaired Student's *t*-test for. NS, not significant. Data are represented as mean ± s.e.m.

6. The evidence for the TNFa involvement in EVP-driven NAFLD is highly intriguing, although not unexpected. However, given the existing data, it is difficult to exclude a possibility that TNFa could also be released by cancer cells, and not only from KCs. This could be easily verified.

Authors: We thank the reviewer for this great point. To determine whether TNFα is secreted by tumor cells, we performed ELISA on the EVP-depleted CM following EVP isolation. Interestingly, TNFα was not detected in the CM (**Response to reviewers Figure 11**, also included in the manuscript as **Extended Data Figure 8j**). Furthermore, we performed MS proteomics on the EVPs derived from both B16F10 and K7M2 cells, and TNFα protein was not detected (raw proteomics data can be provided upon request), consistent with our previous studies (Hoshino *et al.*, 2020; Peinado *et al.*, 2012). Taken together, these data exclude the possibility that TNFα was released by tumor cells either directly into the CM or in the tumor-derived EVPs.

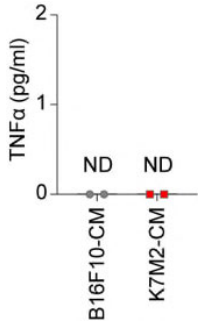

Response to reviewers Figure 11. TNFα is not produced by tumor cells. TNFα ELISA on EVP-depleted conditioned medium from B16F10 and K7M2 cells. n=2 independent experiments. ND, not detected.

7. There are also some questions related to the experimental side of the study.

(i) In several experiments the effects of EVPs are compared to untreated controls, PBS or other unspecified controls. This is not ideal, as it does not address the specificity of the EVP sources. Control EVPs (e.g. from normal cells, or blood borne) should be more widely used as controls.

Authors: We thank the reviewer for this important point. As shown above in **Response to reviewers Figure 10**, additional experiments were performed to demonstrate that the effects of tumor-derived EVPs on liver metabolism are specific to the tumor and not induced by EVPs isolated from non-malignant cells. Specifically, we used EVPs isolated from primary bone-derived osteoblasts, as these are the normal counterpart and cell of origin of osteosarcoma K7M2, as the normal control EVPs for osteosarcoma K7M2-CL-EVPs. Primary osteoblast EVPs were used for both *in vivo* education and *ex vivo* treatment of precision-cut liver slices (**Response to reviewers Figure 10c**). Remarkably, osteoblast EVPs did not induce fatty liver formation *in vivo* or *ex vivo*.

For B16F10-CL-EVPs, unfortunately, melanocyte (the normal counterpart of B16F10) -derived EVPs (Melan-a-CL-EVPs) could not be used for *in vivo* education or *ex vivo* liver slice treatment. Melan-a, a non-malignant melanocyte cell line, requires media containing 12-*O*-tetradecanoylphorbol-13-acetate (TPA) for growth, which can itself induce *Tnf* expression (data shown in the manuscript **Extended Data Figure 9e,i,j**).

We also included bone- and skin-tissue explant (TE)-EVPs as normal controls for K7M2- and B16F10-tumor explant EVPs, respectively. However, due to the low amount of EVPs secreted by normal tissues (e.g., ~7

µg and 30 µg of bone- and skin-TE-EVPs per mouse, respectively), it is difficult to isolate enough material for long-term *in vivo* education. Therefore, we used these bone- or skin-TE-EVPs as controls in *in vitro* experiments with Kupffer cells or in precision-cut liver slices *ex vivo*. Similar to osteoblast-EVPs, neither bone- nor skin-TE-EVPs induced *Tnf* expression in Kupffer cells, or fatty liver formation in liver slices (**Response to reviewers Figure 10b,d**). In contrast, the EVPs from tumor cell lines and tumor tissue explants of both B16F10 and K7M2 models were all able to induce fatty liver generation *in vivo* in educated mice (data shown in the manuscript **Figure 2j**,**k** and **3a**,**b**) and *ex vivo* in the precision-cut liver slices (**Response to reviewers Figure 10c**,**d**). Taken together, these data demonstrate that tumor EVPs, but not EVPs derived from normal tissues/cells, can specifically reprogram liver metabolic function. In addition, we also showed that osteoblast-EVP education did not enhance doxorubicin-induced cardiotoxicity compared to K7M2-CL-EVPs (**Response to reviewers Figure 7c**,**d**).

(ii) The vast majority of the experimental analysis is based on two murine cancer cell lines that have been in passage for decades (e.g. B16F10). Since there are no obvious immune components of the process observed, at least as presented, it is unclear why some of the experiments could not have been performed with patient-derived human cancer cells, PDX grafts, organoids, or in transgenic systems that would offer a more faithful, diverse and molecularly defined reflection of cancer biology. At least some of these possibilities could probably be considered.

Authors: We thank the reviewer for these great suggestions. As shown above, in response to the reviewer's Question 2, we included melanoma GEMM, the human melanoma cancer cell line SK-MEL-192, and primary osteosarcoma PDX isolated from 7 different osteosarcoma patients (**Response to reviewers Figure 4a-c**). Importantly, we found that regardless of the species or model, tumors with extra-hepatic metastatic tropism dysregulate lipid metabolism and induce fatty liver generation.

(iii) Micrometastases in the liver could often be overlooked. Can the authors rule out the effects of micrometastatic disease?

Authors: We thank the reviewer for this critical observation. To rule out the effects of micrometastasis on the liver, we thoroughly analyzed the livers and lungs (the expected metastatic site) of the two major tumor models, B16F10 and K7M2, studied in this work. We performed qRT-PCR to measure the expression of a melanoma-specific gene, *Trpm1*, in the livers and lungs of B16F10 tumor-bearing mice. Melanoma-specific *Trpm1* expression was detected in the lungs, but not in the livers of B16F10 tumor-bearing mice, or either organ of PBS-injected controls (**Response to reviewers Figure 12a**, also included in the manuscript as **Extended Data Figure 1e**). Since there are no osteosarcoma-specific genes that could be used to measure K7M2 cell dissemination by qRT-PCR, we generated a K7M2 cell line expressing mCherry (K7M2-mCherry) and implanted this cell line into mice via intra-tibial injection (as we had done for wild type K7M2 cells). Four weeks post tumor cell implantation, livers and lungs were collected for qRT-PCR to quantify tumor-specific *mCherry* gene expression. Importantly, *mCherry* gene expression was only detected in the lungs, but not in the livers of K7M2-mCherry tumor bearing mice, or either organ of PBS-injected controls (**Response to reviewers Figure 12b**, also included in the manuscript as **Extended Data Figure 1e**). Taken together, these data rule out the effects of micrometastatic disease in liver metabolic dysregulation.

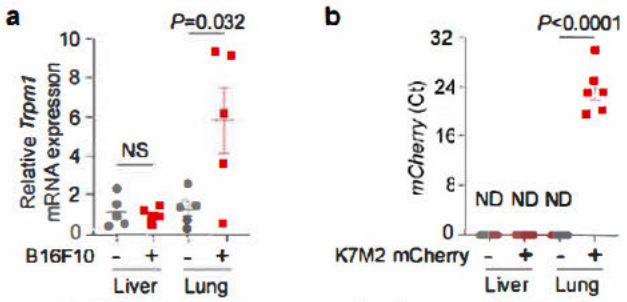

Response to reviewers Figure 12. Micrometastases can be detected in the lungs but not livers of B16F10- and K7M2-Tb mice. a,b, qRT-PCR analysis of *Trpm1* and *mCherry* gene expression in the livers and lungs from B16F10-Tb (a) and K7M2-mCherry-Tb (b) mice, respectively, compared to their PBS-injected controls. n=5 per group for B16F10-Tb model. n=4 control and n=6 K7M2-mCherry-Tb mice. *P* values were determined by the two-tailed, unpaired Student's *t*-test. Data are represented as mean ± s.e.m. NS, not significant; ND, not detected.

(iv) Among factors that regulate the pathogenesis of NAFLD and NASH are inflammatory cells that could be expected to be recruited by cytokines recorded by the authors in KCs following EVP exposure. Is the influx of inflammatory myeloid cells a part of the EVP effects?

Redacted text

(v) It might be useful to determine how may cancer EVPs are present in the circulation and compare this to the amount being injected during education experiments.

Authors: Following the reviewer's suggestion, we performed nanoparticle tracking analysis (NTA) of the EVPs isolated from the plasma of B16F10 and K7M2 tumor-bearing models, and EVPs from B16F10 and K7M2 cell lines. There was an average of 7×10^9 and 4×10^9 EVPs in 1 ml of plasma from B16F10 and K7M2 tumor-bearing mice, respectively, versus 2×10^9 of EVPs in 1 ml of control plasma (Response to reviewers Figure 13a,b, also included in the manuscript as Extended Data Figure 3b). An average of 4×10^9 and

0.8×10^9 of EVPs were detected in 10 μg of B16F10 and K7M2 cell-derived EVPs, respectively, indicating that the amount of injected EVP particles during education experiments was lower than that of circulating EVPs in tumor-bearing mice, and thus the functional effects on liver metabolism we observed upon tumor EVP education were not due to delivering an "overdose" of EVPs.

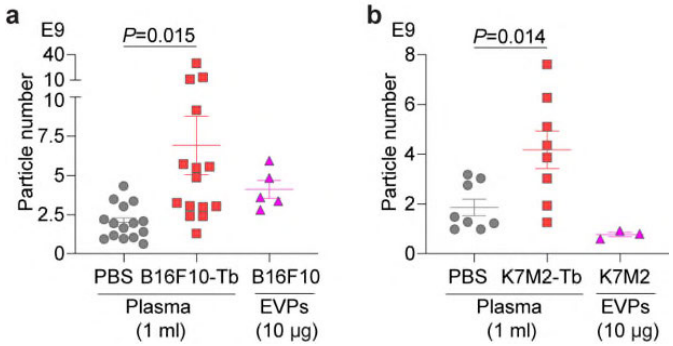

Rebuttal Figure 13. Nanoparticle tracking analysis of EVPs in the circulation of tumor-bearing mice or of EVPs derived from tumor cells. a,**b**, Statistical analysis of the particle numbers in 1 ml of plasma from B16F10-Tb (**a**) and K7M2-Tb (**b**) mice, compared to their PBS-injected controls, as well as in 10 μg of EVPs derived from B16F10 (**a**) and K7M2 (**b**) cells. n=15 control and B16F10-Tb mice; n=8 control and K7M2-Tb mice; n=5 and n=3 independent experiments for EVPs derived from B16F10 and K7M2 cells, respectively. *P* values were determined by the two-tailed, unpaired Student's *t*-test. Data are represented as mean ± s.e.m. Tb, tumor-bearing.

7. Minor concerns:

(i) The manuscript, while well written, is inundated with unnecessary abbreviations (e.g. KC, LD, PCLS, B16F10-Tb and may others). This makes the reading of the paper difficult.

Authors: The abbreviations have been spelled out in the manuscript. KC (short for Kupffer cells) was kept since it has been widely used in the literature.

(ii) The nature of controls should be specified in all figures.

Authors: The nature of controls has been specified in all figures in the revised manuscript.

(iii) There is a vast literature on EV homing to the liver upon exogenous injection, which may be worth acknowledging beyond authors own work.

Authors: We apologize for the omission and thank the reviewer for pointing this out. We have now included additional references on EVP homing to the liver from other groups (Xie et al., 2022; Zhang et al., 2017)

Referee #2 (Remarks to the Author):

The view of cancer pathogenesis has expanded from cell-intrinsic to cell-extrinsic regulation, and cancer is now viewed as a systemic disease. Tumors can deregulate the physiology of distant organs without metastasizing to that organ. Little is known about how tumors reprogram systemic physiology and what

are the consequences of these systemic effects on the host. The study by Wang et al. provides novel insights into these fundamental biological questions.

This study describes a new mechanism of reprogramming liver metabolism by tumors that do not metastasize to the liver. The authors show that tumor-derived extracellular vesicles and particles (EVPs) reprogram liver metabolism by carrying fatty acids (cargo) to Kupffer cells, which induces the secretion of TNF-alpha. This process of EVP education creates a pro-inflammatory milieu that suppresses fat metabolism and oxidative phosphorylation in the liver and leads to fatty liver formation. Through genetic studies, the authors demonstrate the function of EVPs in fatty liver formation and their impact on anti-cancer drug metabolism. Complementary to the experimental studies, the authors show that the fatty liver phenotype is also observed in pancreatic cancer patients with tumor-free livers. These novel mechanistic studies reveal a new facet of systemic regulation by tumors and are timely. These studies can have a high clinical impact and can inform treatment decisions. The study is well-controlled with rigor and statistical considerations. A few comments that need to be addressed are listed below.

Authors: We appreciate the reviewer's positive assessment of our work. In response to the reviewer's thoughtful comments, we have performed numerous additional experiments to address the reviewer's concerns.

The clinical data includes patients with a fatty liver at diagnosis who later developed extra-hepatic metastasis. Does fatty liver formation after EVP injection increase the risk of extra-hepatic metastasis in mouse models? If fatty liver is first induced by EVP education, followed by injection of cancer cells via circulation (e.g., via the tail vein), this point can be experimentally tested.

Redacted text

Redacted text and figure

It will be interesting to know how TNF alpha regulates lipid accumulation in hepatocytes in EVP injected mice. Is it increased synthesis of lipid droplets or inhibition of lipid catabolism, or both?

Authors: We thanks the reviewer for this great comment. To determine if TNFα increases lipid synthesis or suppresses lipid catabolism, we performed RNA-seq on primary hepatocytes 24 h post TNFα treatment.

Gene set enrichment analysis (GSEA) of the gene expression profiles, using the Gene Ontology gene sets, revealed that gene sets associated with lipid catabolism were significantly downregulated (Response to reviewers Figure 15, also included in the manuscript as Extended Data Figure 8k). These data indicate that tumor-EVP induced Kupffer cell secretion of TNFα resulted in lipid accumulation in hepatocytes due mainly to inhibition of lipid catabolism.

NAME	NES	NOM *p* value
GOBP_CELLULAR_LIPID_CATABOLIC_PROCESS	-1.47398	0.009456265
GOBP_FATTY_ACID_BETA_OXIDATION	-1.46986	0.019522777
GOBP_LIPID_CATABOLIC_PROCESS	-1.46491	0.007594937
GOBP_NEUTRAL_LIPID_METABOLIC_PROCESS	-1.46388	0.033254158
GOBP_FATTY_ACID_CATABOLIC_PROCESS	-1.46103	0.024774775
GOBP_NEUTRAL_LIPID_CATABOLIC_PROCESS	-1.38641	0.045553144
GOBP_GLYCEROLIPID_CATABOLIC_PROCESS	-1.38472	0.035955057

Response to reviewers Figure 15. TNFα downregulates lipid catabolism-associated pathways. GSEA of all differentially expressed genes, ranked based on the sign of log2FC*-log10(*p* value), in hepatocytes 24 h post treatment with recombinant murine TNFα protein (25 ng/ml), compared to PBS control, using Gene Ontology gene sets. Shown are downregulated lipid catabolism-associated gene sets. NES, normalized enrichment score. NOM *p*-value, nominal *p*-value.

Do acute phase proteins (APP) get induced in the hepatocytes during fatty liver formation in EVP-injected mice? APP upregulation could be an early indicator of cachexia. On a related point, is there a visible impact of such liver reprogramming on skeletal muscle or adipose tissue? In other words, is cachexia another systemic effect associated with fatty liver formation?

Redacted text

Redacted text and figure

The authors show that TNF-alpha neutralization in mice reverses lipid droplet accumulation in the liver. Does TNF-blockade reverse the impaired drug metabolism through CYPs? This data could have important treatment implications.

Authors: We thank the reviewer for this great comment. To address this question, we quantified *Cyp* gene expression by qRT-PCR in the primary hepatocytes isolated from both B16F10-Tb and B16F10-CL-EVP-educated mice after anti-TNFα treatment. We found that TNFα blockade rescued *Cyp* gene expression in hepatocytes from both B16F10-Tb and B16F10-CL-EVP-educated mice (Response to reviewers Figure 17a,b, also included in the manuscript as Figure 6b,c). More importantly, the capacity of B16F10-Tb livers and B16F10-CL-EVP-treated precision-cut liver slices to metabolize drugs was also rescued after TNFα blockade (Response to reviewers Figure 17c,d, also included in the manuscript as Figure 6e,f). These findings suggest that timely and restricted TNFα blockade, potentially concurrent with chemotherapy administration, may enhance the efficacy of chemotherapy by restoring liver function.

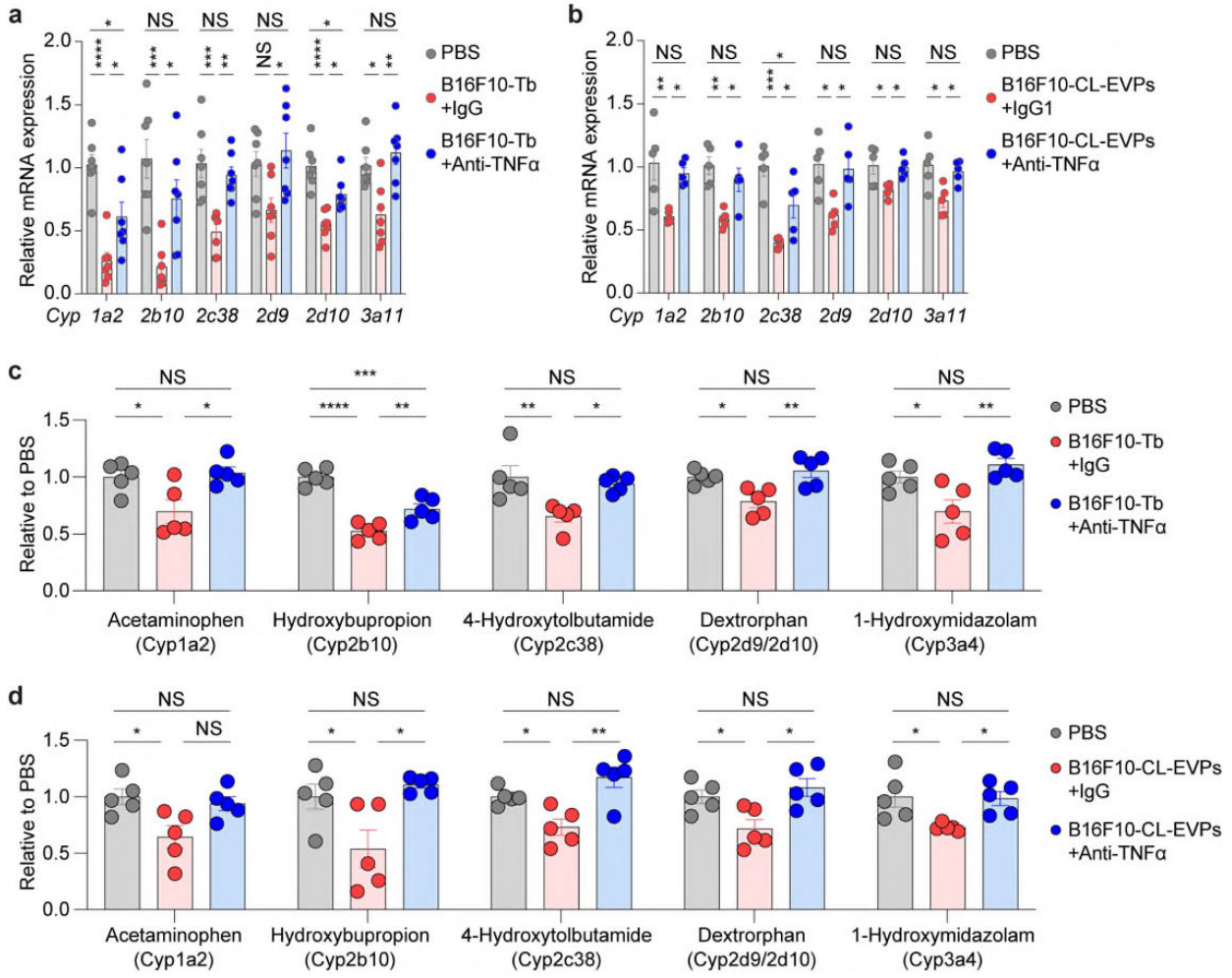

Response to reviewers Figure 17. TNFα blockade rescues CYP-mediated drug metabolism in both tumor-bearing and tumor-EVP-educated mice. a,**b**, qRT-PCR analysis of *Cyp* gene expression in primary hepatocytes isolated from B16F10-Tb mice (**a**) and B16F10-CL-EVP-educated mice (**b**) treated with anti-TNFα antibody or IgG1 isotype control, compared to their respective PBS-injected controls. n=7 mice per group for (**a**) and n=5 mice per group for (**b**). **c**,**d**, Drug metabolizing activity of the core Cyp450 enzymes in precision-cut liver slices from PBS-injected mice, and B16F10-Tb mice treated with anti-TNFα antibody or IgG1 isotype control (**c**), or naïve mice pre-treated with PBS or 10 μg/ml of B16F10-CL-EVPs with co-treatment of anti-TNFα antibody (20 μg/ml) or IgG1 isotype (20 μg/ml) control for 24 h (**d**). n=5 mice per group. *P* values were determined by one-way ANOVA with post hoc Tukey's test. NS, not significant. Data are represented as mean ± s.e.m.

Is the fatty liver phenotype observed in allografts/genetic models of pancreatic cancer? This data would cross-validate the clinical observations.

Authors: In response to the reviewer's comment, we examined a genetic murine model of tamoxifen-inducible, spontaneous pancreatic ductal adenocarcinoma (PDAC), the KPC mice (*Kras*^{tm4Tyj} *Trp53*^{tm1Brn} Tg[Pdx1-cre/Esr1*]#Dam/J) (Maddipati and Stanger, 2015). Briefly, *Trp53* excision was induced in pups via lactation upon administration of tamoxifen (6 mg/mouse) via oral gavage to the dam. Mice carrying the *Kras*^{G12D} mutation in one allele (*Kras*$^{WT/G12D}$) developed pancreatic intraepithelial neoplasia (PanIN) lesions

at 8-10 weeks of age, which progressed into local PDAC at 10-14 weeks and invasive PDAC at 15-18 weeks, associated with distant metastasis to several sites including lymph nodes, liver, lungs, diaphragm, and spleen. Since liver metastasis can always be detected in 20-week tumor-bearing mouse, the liver of the 14-week tumor-bearing mouse is considered as the pre-metastatic niche (PMN) (**Response to Reviewers Figure 18a**, also included in the manuscript as **Extended Figure 2j**). However, lipid droplet accumulation (fatty liver) was not observed in the PMN liver of 14-week-old tumor-bearing mice (**Response to Reviewers Figure 18b**, also included in the manuscript as **Extended Figure 2k**). We speculate that in the genetic murine model of PDAC, tumor progression leads to liver PMN formation, which precludes the generation of fatty liver. This finding supports our hypothesis that tumors and EVPs shed from tumors with extrahepatic metastatic tropism induce fatty liver generation, as we have found multiple non-liver metastatic cancer models, including melanoma, breast cancer and osteosarcoma, which can all induce fatty liver formation. In contrast, liver-metastatic tumors and their EVPs which carry distinct cargo induce pre-metastatic niche formation in the liver. We further discussed the difference between fatty liver formation and PMN in the manuscript Discussion section (Page 17).

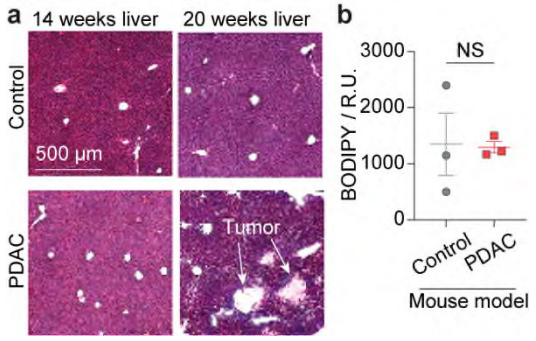

Response to Reviewers Figure 18. Fatty liver is not induced in the PMN liver of murine genetic model of PDAC. a, Representative H&E staining images of the livers from genetic pancreatic cancer mouse model. Liver metastasis was observed in 20-week, but not 14-week tumor bearing mice. Scale bar, 500 μm. **b**, Statistical analysis of BODIPY staining of the livers from 14-week PDAC tumor-bearing mice, compared to non-PDAC controls. n=3 mice per group. *P* values were determined by the two-tailed, unpaired Student's *t*-test. NS, not significant. Data are represented as mean ± s.e.m.

A more detailed histological staining and quantitation of the fatty liver phenotype (Fig. 1 and Extended data 1) longitudinally in mouse models would clarify the kinetics, extent, and severity of the phenotype.

Authors: In response to the reviewer's comment, we performed BODIPY staining on the livers from tumor-bearing mice 2 or 3 weeks post tumor cell implantation. These timepoints were chosen as they correspond to PMN formation in the lungs for melanoma (B16F10) and breast cancer (4T1) (2 weeks), and micrometastasis formation in the lungs for osteosarcoma (K7M2) (3 weeks), respectively. Furthermore, the 2-week timepoint was also chosen for low metastatic B16F1 melanoma and non-metastatic 67NR breast cancer models. Interestingly, we found that fatty liver generation was already evident at these early timepoints, although the lipid droplet accumulation was lower compared to the endpoint (**Response to Reviewers Figure 19**, for reviewers only). These data suggest the fatty liver generation is initiated early during tumor progression and lipid droplets accumulate as the tumor progresses.

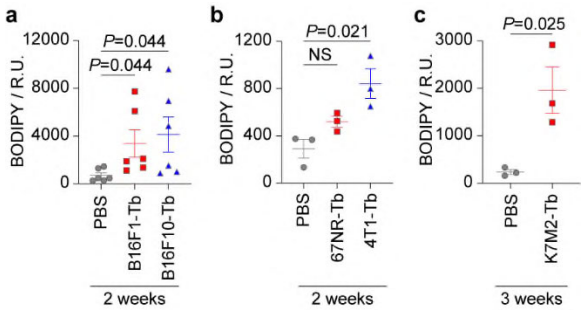

Response to Reviewers Figure 19. Fatty liver is induced at early stages of tumor progression in murine cancer models without liver metastasis. a,b,c Statistical analysis of the BODIPY staining of the livers from 2-week melanoma B16F1- and B16F10-Tb mice (**a**), 2-week breast cancer 67NR- and 4T1-Tb mice (**b**), and 3-week osteosarcoma K7M2-Tb mice (**c**), compared to PBS-injected controls. n=6 mice per group for melanoma models, n=3 mice per group for breast cancer and osteosarcoma models. *P* values were determined by the two-tailed, unpaired Student's *t*-test. Data are represented as mean ± s.e.m.

The fluorescence-based EVP tracking experiment in-vivo is elegant. Can the authors track where the EVP cargo gets taken up besides the liver?

Authors: We thank the reviewer for the compliment. Following the reviewer's suggestion, we labeled both the B16F10-CL-EVPs and K7M2-CL-EVPs with Cell-Vue NR815 dye, and intra-venously injected the EVPs into mice. Twenty-four hours later, mice were euthanized, and organs and tissues were collected for whole organ Odyssey near-infrared imaging. We found that, in addition to the liver, tumor EVPs from both models were also taken up by lung, spleen, bone, adrenal gland, lymph node and brown adipose tissue (BAT), but not brain, pancreas or TA muscle (**Response to Reviewers Figure 20**, for reviewers only). As addressed in response to the reviewer's first comment, the EVP-enhanced extrahepatic metastasis might be due to direct targeting and functional reprogramming of those organs and tissues, including the lung and immune organs (such as spleen, lymph node and bone). The potential tumor EVP-induced functional reprogramming of those tissues and organs warrants further investigation to dissect additional systemic effects of cancer.

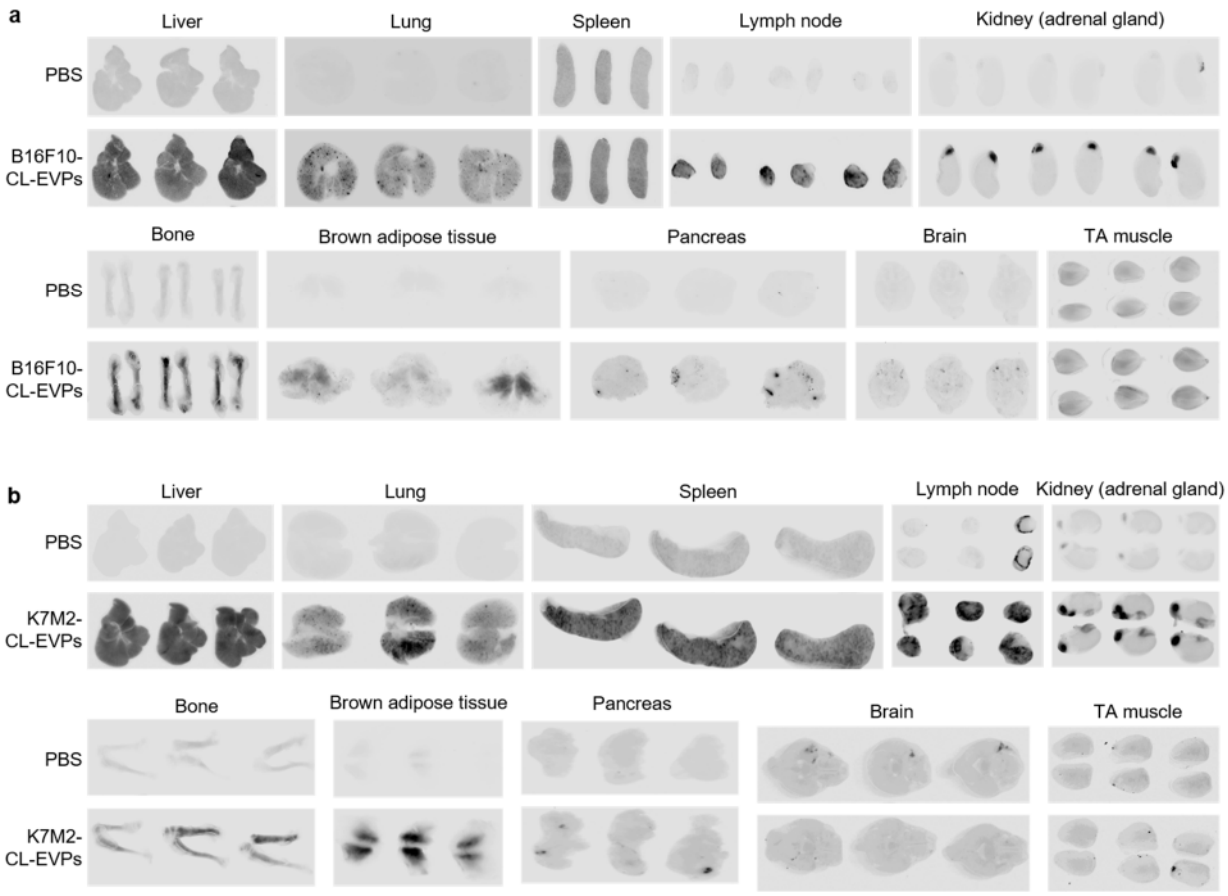

Response to Reviewers Figure 20. Biodistribution of cancer cell-derived EVPs in different tissues and organs of mice. a,**b**, Representative Odyssey images of tissues and organs, including liver, lungs, spleen, lymph node, kidney (adrenal gland), bone, brown adipose tissue, pancreas, brain and TA muscle, from mice 24 h post intravenous injection of 10 µg of CellVue NIR815-labeled B16F10-CL-EVPs (**a**) or K7M2-CL-EVPs (**b**), and their mock PBS-injected controls. n=3 mice per group.

An interesting question is what dictates whether the EVPs will form a pre-metastatic niche (PMN) or generate fatty liver in the liver microenvironment. The authors have mentioned this point in the Discussion section, but a more detailed discussion will clarify this important distinction.

Authors: We thank the reviewer for this great comment. We have discussed the difference between liver PMN and fatty liver formation in more detail in the manuscript Discussion section (Page 17).

Referee #3 (Remarks to the Author):

The study submitted by Dr. Lyden and colleagues investigated the role of tumor-derived EVPs in the development of fatty liver and demonstrated its underlying mechanism and the clinical implication by focusing on the drug metabolism capacity. First, the authors used B6F10 and K7M2 lung metastasis models and found gene expression profiles are different in the tumor-free liver of tumor bearing mice compared to the normal liver and fatty liver was induced in tumor-bearing mice. The study further identified that tumor-derived EVP is responsible for fatty liver development. Secreted EVPs were mainly

uptaken by Kupffer cells. Also, the study revealed that PDAC patients without liver metastasis developed fatty liver, supporting the findings from mouse experiments. The study also investigated the underlying mechanisms. EVP stimulated Kupffer cells to produce TNFa through TLR4 and this TNFa induced fatty liver. Lastly, the study showed that drug metabolism capacity was decreased by tumor-derived EVPs. These results are very interesting and the experimental approaches are very logic. Especially, the experiment using Rab27a silencing in tumor cells is a good approach. Overall, the study is very interesting. One question is whether decreased drug metabolism by tumor-derived EVPs is associated with fatty liver or whether fatty liver development is necessary for decreasing drug metabolism is unclear. If these are independent, what is the clinical implication of tumor-derived EVP-induced fatty liver?

Authors: First, we appreciate the reviewer's positive assessment of our work. In response to the reviewer's question regarding the association between tumor EVP-induced fatty liver and decreased drug metabolism, we treated primary hepatocytes with TNFα, and found that TNFα treatment was sufficient to induce lipid droplet accumulation and suppress drug metabolism-associated *Cyp* enzyme gene expression in primary hepatocytes (data from the manuscript **Figure 5c** and **Figure 6a** are shown here as **Response to Reviewers Figure 21a,b**). TNFα-treated hepatocytes were also subjected to RNA-seq, and Gene set enrichment analysis (GSEA) of differentially expressed genes revealed that the Drug Metabolism Cytochrome P450 gene set was significantly downregulated in the hepatocytes after TNFα treatment (**Response to Reviewers Figure 21c**, also included in the manuscript as **Figure 6d**). Thus, lipid droplet accumulation in liver/primary hepatocytes is associated with altered drug metabolism downstream of TNFα. Interestingly, TNFα blockade not only dramatically reduced fatty liver generation (data from the manuscript **Figure 5e,f** are shown here as **Response to Reviewers Figure 21d,e**), but also reversed *Cyp* gene expression in the livers of tumor-bearing and tumor EVPs educated mice (**Response to Reviewers Figure 21f,g**, also included in the manuscript as **Figure 6b,c**). Furthermore, we analyzed drug metabolism *ex vivo* in precision-cut liver slices. We found that TNFα blockade was sufficient to reverse drug metabolism impairment in liver slices from tumor-bearing mice or tumor EVP-treated precision-cut liver slices (**Response to Reviewers Figure 21h,i**, also included in the manuscript as **Figure 6e,f**). Therefore, our data indicate that fatty liver disease and impaired drug metabolism are interconnected and regulated/induced by the pro-inflammatory cytokine TNFα. Consistent with our findings, prior studies have shown that impaired expression and activity of drug metabolizing CYP450 enzymes is observed in patients with fatty liver disease (Cobbina and Akhlaghi, 2017; Woolsey et al., 2015). Taken together, our findings described here in a variety of tumor models indicate that fatty liver formation and impaired drug metabolism are closely linked mechanistically and are both regulated by the pro-inflammatory cytokine TNFα.

Indeed, it is technically difficult to dissociate fatty liver and drug metabolism, since currently there are no FDA approved drugs for treating fatty liver disease (Rau and Geier, 2021). Clinically, timely and restricted blockade of TNFα can potentially reverse both fatty liver and drug metabolism impairment concurrently.

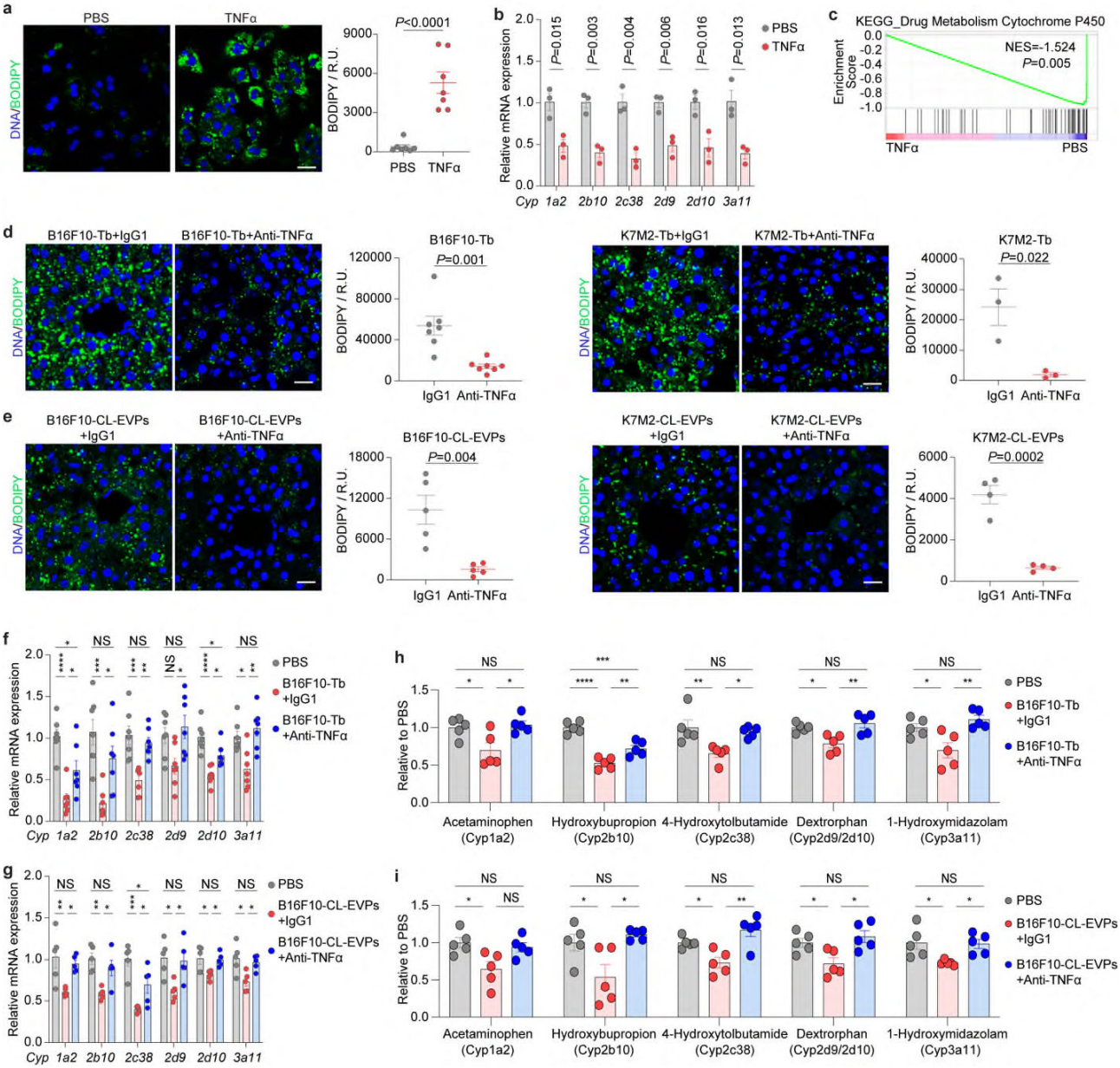

Response to Reviewers Figure 21. TNFα blockade reverses fatty liver formation and impaired CYP-mediated drug metabolism in B16F10 tumor-bearing and B16F10-CL-EVP-educated mice. a, Representative images (left) and associated statistical analysis (right) of BODIPY staining of the primary hepatocyte 48 h post treatment with recombinant murine TNFα protein (25 ng/ml), or PBS control. n=7 independent experiments. **b**, qRT-PCR analysis of the expression level of *Cyp* genes in the primary hepatocyte treated with control PBS or recombinant murine TNFα protein (25 ng/ml) for 24 h. n=3 independent experiments. **c**, GSEA of gene expression profiles in the 24-h TNFα-treated murine primary hepatocytes, compared to PBS-treated controls, showing downregulation of drug metabolism cytochrome P450 signaling pathway. n=3 per group. **d**,**e**, Representative images (left) and statistical analysis (right) of BODIPY staining of the livers from B16F10- and K7M2-Tb mice (**d**), and B16F10-CL-EVP- and K7M2-CL-EVP-educated mice (**e**), treated with anti-TNFα antibody or IgG1 isotype control. For B16F10-Tb model, n=7 mice per group. For K7M2-Tb model, n=3 mice per group. For B16F10-CL-EVP education model, n=5 mice

per group. For K7M2-CL-EVP education model, n=4 mice per group. **f**,**g**, qRT-PCR analysis of the expression level of *Cyp* genes in the primary hepatocytes isolated from B16F10-Tb mice (**f**) and B16F10-CL-EVP-educated mice (**g**) treated with anti-TNFα antibody or IgG1 isotype control, compared to their respective PBS-injected controls. n=7 mice per group for (**f**) and n=5 mice per group for (**g**). **h**,**i**, Drug metabolizing activity of the core Cyp450 enzymes in the precision-cut liver slices sectioned from PBS-injected mice, and B16F10-Tb mice treated with anti-TNFα antibody or IgG1 isotype control (**h**), or naïve mice pre-treated with PBS or 10 μg/ml of B16F10-CL-EVPs with co-treatment of anti-TNFα antibody (20 μg/ml) or IgG1 isotype (20 μg/ml) control for 24 h (**i**). n=5 mice per group. *P* values were determined by the two-tailed, unpaired Student's *t*-test (**a**,**d**,**e**), or multiple unpaired t-test (**b**), or one-way ANOVA with post hoc Tukey's test (**f**-**i**). NS, not significant. Data are represented as mean ± s.e.m.

Specific comments:

1. Figure 1b (and Extended Figure 1e,g). This reviewer agrees that decreased fatty acid metabolism and oxidative phosphorylation could be associated with fatty liver development. However, adipogenesis signature was decreased. Is this in contrast to increased fatty liver? Similarly, in Fig.2d,e, EVP injection decreased adipogenesis signature.

Authors: We thank the reviewer for this insightful comment. We agree with the reviewer that it is indeed intriguing that adipogenesis was downregulated in the livers of both tumor-bearing and EVP-educated mice. Importantly, consistent with and in support of our observation, downregulation of liver adipogenesis signatures has also been observed in patients with fatty liver disease (Juhling et al., 2021; Skat-Rordam et al., 2021; Zhang et al., 2022).

We hypothesize such downregulation of adipogenesis signatures is due to increased levels of TNFα in the livers of tumor-bearing mice and tumor-EVP-educated mice. This hypothesis is supported by published studies showing that TNFα can functionally suppress adipogenesis signaling pathways in the adipose tissue itself (Cawthorn et al., 2007). To test this hypothesis, we performed RNA-seq on primary hepatocytes 24 h post TNFα treatment. GSEA of the RNA-seq data revealed that adipogenesis was indeed downregulated in TNFα-treated primary hepatocytes, suggesting that TNFα is sufficient to downregulate adipogenesis signatures in these cells, as well as induce lipid droplet accumulation. These data indicate that these two processes occur simultaneously (manuscript **Figure 5c,** and **Response to Reviewers Figure 22** for reviewers only). However, the potential functional interaction between down-regulation of adipogenesis signature genes and fatty liver formation (due mainly to decreased lipid catabolism pathways as shown above in **Response to reviewers Figure 15** that included in the manuscript as **Extended Data Figure 8k**) requires further investigation and is discussed in the manuscript (page 16: "However, the mechanisms governing the crosstalk between adipogenesis and lipogenesis during fatty liver generation, and whether the dysregulation of adipogenesis signature genes directly impacts lipid droplet accumulation during cancer progression remain unknown and require further investigation.").

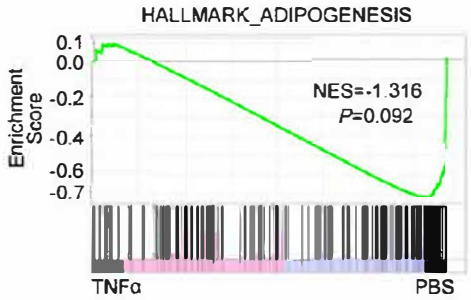

Response to Reviewers Figure 22. TNFα treatment inhibits adipogenesis signature in the murine primary hepatocyte. Primary hepatocytes isolated from naïve mice were treated with control PBS or recombinant murine TNFα protein (25 ng/ml) for 24 h, and then collected for RNA extraction followed with RNA-seq. GSEA of gene expression profiles in the TNFα-treated murine primary hepatocytes, compared PBS-treated controls, showing downregulation of adipogenesis signature. n=3 per group.

2. Figure 1J showed all pancreatic cancer patients had fatty liver. The text mentioned BMIs are same between cancer patients and control patients. Figure 1J included 4 cancer patients and 5 control patients, but Supplementary Table 5 included 12 controls and 8 PDAC patients. The sample number for fatty liver evaluation should increase to gain a sufficient power, and reassessment of BMI should strongly be recommended. Otherwise, the data are highly biased. Also, BMI could affect fatty liver. For example, control patients with high BMI (e.g. BMI>30) are highly expected having fatty liver.

Authors: We thank the reviewer for these thoughtful comments. Indeed, the numbers of PDAC patients and control subjects presented in the original Figure 1J are lower than those in the Supplementary Table 5. The reason for the discrepancy is that, for the initial submission, due to limitations in patient liver sample amount and the procedure for sample preparation, livers from the same patient could not be used for both RNA-seq and BODIPY staining simultaneously. The number of patient liver samples listed in the Supplementary Table 5 included all patient samples used for BODIPY staining and RNA-seq.

Following the reviewer's suggestion, we stained with BODIPY on liver samples from 7 additional PDAC patients without liver metastasis (but with extrahepatic metastasis) and 3 additional control subjects with benign lesions. Results confirmed our findings that fatty liver generation was induced/enhanced in the PDAC patients with extrahepatic metastasis relative to controls (Response to Reviewers Figure 23a, also included in the manuscript as Figure 1j).

Furthermore, there is no difference in BMIs between PDAC patients and control subjects used in this study (Response to Reviewers Figure 23b, also included in the manuscript as Extended Data Figure 2l).

Redacted text

Taken together, these data confirmed our conclusion that fatty liver generation was increased in the PDAC patients with extrahepatic metastasis. Patient information was updated accordingly in Supplementary Table 5b, and we also specified which patient's liver was used for RNA-seq and which for BODIPY staining, respectively.

Redacted figure

Response to Reviewers Figure 23. PDAC induces fatty liver generation in cancer patients with extrahepatic metastasis. a, Statistical analysis of BODIPY staining of the livers from PDAC patients without liver metastasis and control subjects with benign lesions. n=11 PDAC patients and n=8 control subjects. b, Statistical analysis of the body mass index (BMI) of PDAC patients without liver metastasis and control subjects with benign lesions. n=16 PDAC patients and n=14 control subjects.

Redacted text

values were determined by the two-tailed, unpaired Student's *t*-test. NS, not significant. Data are represented as mean ± s.e.m.

3. Figure 5j suggested PA in EVPs induced TNFα through TLR4. However, Lancaster et al (PMID: 29681442) reported that TLR4 is not a receptor for palmitate. How can the authors explain it?

Authors: We thank the reviewer for highlighting this study. We agree that TLR4 is not a direct receptor for palmitate as shown by Lancaster *et al* (Lancaster et al., 2018). However, both these authors' work and ours suggested that TLR4 is functionally required for PA-induced inflammatory signaling activation in macrophages. Specifically, Lancaster *et al* showed that PA treatment can activate JNK signaling in bone marrow-derived macrophages (BMDMs) from wild type mice, but not *Tlr4*$^{-/-}$ mice. Moreover, they showed that PA induces JNK phosphorylation in BMDMs from control C3H/HeN mice, but not C3H/HeJ mice, which harbor a mutation in the TIR domain that results in normal levels of expression of TLR4, albeit a dysfunctional one. Furthermore, the authors showed that pre-treatment with TAK, a TLR4 inhibitor, abolishes PA-induced inflammation in wild type BMDMs. Consistently, we also found that when the liver resident macrophages, Kupffer cells (KCs), were pre-treated with TAK, PA did not induce TNFα expression in KCs (data shown in the manuscript Extended Data Figure 9c, and detailed protocol for TAK treatment is described in the Materials and Methods section). Indeed, Lancaster *et al* (Lancaster *et al.*, 2018) demonstrated that TLR4-induced metabolic reprogramming of the BMDMs is a pre-requisite for long chain saturated fatty acid PA initiation of inflammatory signaling.

Moreover, Lancaster *et al* performed their studies in BMDMs while we studied liver resident macrophages, KCs. The different source of macrophages might contribute to differences in functional outcomes. To avoid confusion, we modified our conclusion in the manuscript to: "These findings suggest that EVP-packaged PA activates inflammatory pathways in KCs and that this process depends on Tlr4 functional integrity in recipient cells" (on Page 13).

4. The authors tested several drugs and showed drug metabolism for those drugs were decreased. What is the metabolism of anti-cancer chemo drugs in hepatocytes affected by tumor-derived EVPs? May these drugs cause more toxicity to host or cancer?

Authors: We thank the reviewer for the insightful comments. In response to these comments, we tested the toxicity of two anti-cancer chemotherapy drugs, dacarbazine and doxorubicin. These chemotherapeutics are widely used to treat melanoma and osteosarcoma, respectively, and can be metabolized by CYP enzymes (Bagdasaryan *et al.*, 2022; Lewis *et al.*, 2007; Reid *et al.*, 1999).

Chemotoxicity was tested *in vivo* in both the B16F10-CL-EVP and the K7M2-CL-EVP education models. In the B16F10-CL-EVP education model, mice were intra-venously injected with either PBS control or 10 μg of B16F10-CL-EVPs every other day for 4 weeks to induce fatty liver generation, then intra-peritoneally injected with dacarbazine (60 mg/kg) or 0.9% NaCl as control together with intravenous injection of 10 μg of B16F10-CL-EVPs or PBS every other day, 4 times in total. One day after the last injection, retroorbital blood was collected for complete blood count (CBC) (the procedure is illustrated in **Response to Reviewers Figure 24a**, also included in the manuscript as **Extended Data Figure 10c**). We found that tumor EVP-induced fatty liver increased dacarbazine toxicity, as shown by enhanced dacarbazine-induced bone marrow depression (including reduced red blood cells, reticulocytes and hemoglobin) in B16F10-CL-EVP-educated mice (**Response to Reviewers Figure 24b**, also included in the manuscript as **Figure 6g**).

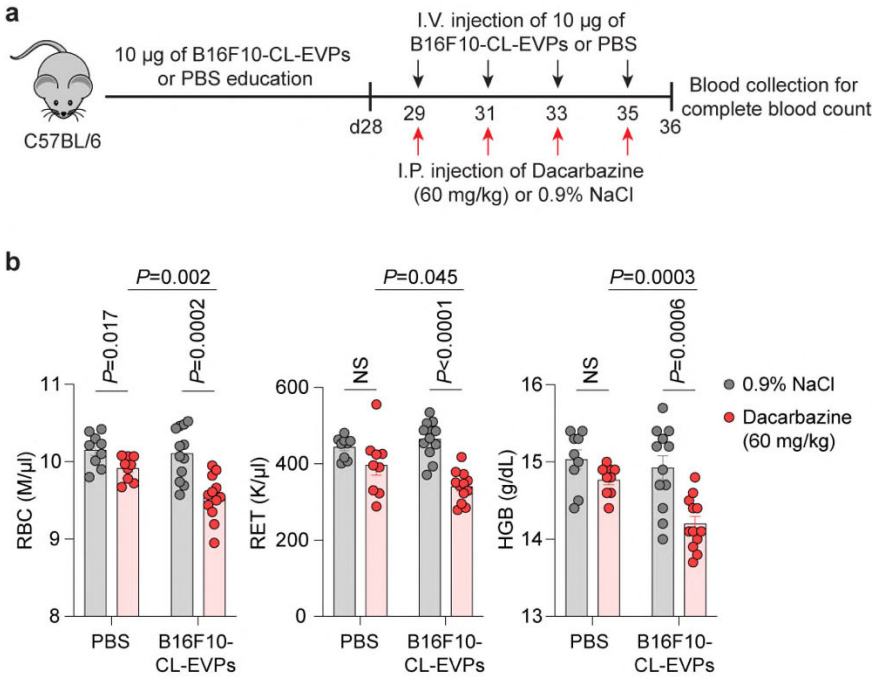

Response to Reviewers Figure 24. Tumor EVP education enhances the toxicity of anti-cancer chemotherapy. a, Schematic illustration of the procedure for measuring chemotherapy toxicity in B16F10-CL-EVP-educated mice. C57BL/6 mice were intravenously injected with PBS or 10 μg of B16F10-CL-EVPs every other day for 4 weeks, then intraperitoneally injected with dacarbazine (60 mg/kg) or 0.9% NaCl together with intravenous injection of PBS or 10 μg of B16F10-CL-EVPs every other day, 4 times in total, and retroorbital blood of the mice was collected 24 h after the last injection for CBC. **b**, Statistical analysis of red blood cells (RBC), reticulocytes (RET) and hemoglobin (HGB) in the PBS- or B16F10-CL-EVP-educated mice after treatment of dacarbazine (60 mg/kg) or 0.9% NaCl. n=9 mice for PBS groups and n=12 for B16F10-CL-EVP groups. *P* values were determined by the multiple unpaired *t*-test and two-tailed, unpaired Student's *t*-test. NS, not significant. Data are represented as mean ± s.e.m. An error was made for the statistical test used in (**b**). The correct test should have been the two-way ANOVA with Fisher's LSD test, and this correction was included in the second revision.

For the K7M2-CL-EVP education model, mice were first intravenously injected with PBS control, 10 µg of primary osteoblast-EVP (Ob-EVPs) control or K7M2-CL-EVPs every other day for 4 weeks to induce fatty liver formation, and then intra-peritoneally injected with doxorubicin (1mg/kg) or DMSO every 24 h together with intravenous injection of PBS, 10 µg of Ob-EVPs or K7M2-CL-EVPs, every other day for 25 days. The cumulative dose of doxorubicin was 25 mg/kg. One day after the last injection, mice were subjected to echocardiography (the procedure is illustrated in **Response to Reviewers Figure 25a**, also included in the manuscript as **Extended Data Figure 10c**). Results showed that K7M2-CL-EVP-induced fatty liver increased doxorubicin toxicity, as shown by enhanced doxorubicin-induced cardiotoxicity (including reduced left ventricular ejection fraction and fractional shortening) at similar heart rates in K7M2-CL-EVP-educated mice, compared to PBS- or Ob-EVP-educated controls (**Response to Reviewers Figure 25b,c**, also included in the manuscript as **Figure 6h** and **Extended Data Figure 10d,e**; and **Supplementary Videos 1-6** showing the echocardiography in the manuscript). These findings demonstrate that tumor EVP-induced fatty liver enhances the toxicity of chemotherapy by suppressing *Cyp* enzymes and thus impairing drug metabolism in the liver, thereby reducing tolerance for anti-cancer chemotherapy in patients.

Unfortunately, we were not able to measure the chemotoxicity to the cancer, given the timeline of tumor growth in these murine models. B16F10 melanoma and K7M2 osteosarcoma reach their maximum allowed size according to our IACUC protocol in 3 and 4 weeks, respectively. Therefore, we could not implant tumor cells first to induce fatty liver followed with multiple doses of chemotherapy.

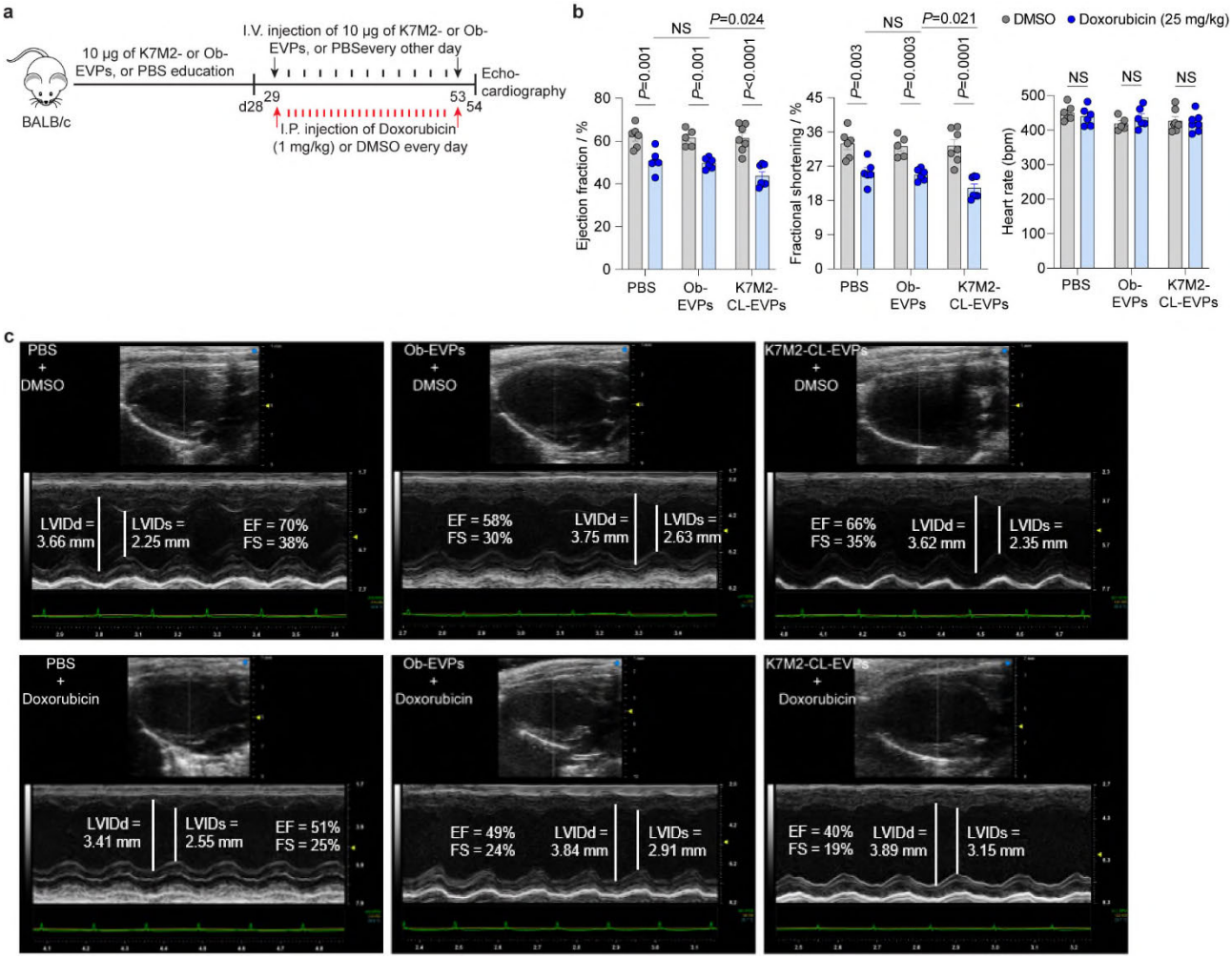

Response to Reviewers Figure 25. Tumor EVP education enhances the toxicity of anti-cancer chemotherapy. a, Schematic illustration of the procedure for measuring chemotherapy toxicity in K7M2-CL-EVP-educated mice. BALB/c mice were intra-venously injected with PBS or 10 μg of primary osteoblast-EVPs (Ob-EVPs) or K7M2-CL-EVPs every other day for 4 weeks, then intra-peritoneally injected with doxorubicin (1 mg/kg) or DMSO every 24 h together with intra-venous injection of PBS or 10 μg of Ob-EVPs or K7M2-CL-EVPs every other day for 25 days. The cumulative dose of doxorubicin was 25 mg/kg, and mice were subjected to echocardiography 24 h after the last injection. **b**, Statistical analysis of the left ventricular ejection fraction (M-mode), ejection shortening (M-mode) and heart rate in the PBS-, or Ob-EVP-, or K7M2-CL-EVP-educated mice after treatment of doxorubicin (cumulative dose of 25 mg/kg) or DMSO. n=6 mice for PBS groups and n=7 mice for K7M2-CL-EVP groups. n=5 and n=6 for DMSO and doxorubicin treated Ob-EVP-educated mice, respectively. **c**, Representative M-mode images of echocardiography for the PBS or Ob-EVP- or K7M2-CL-EVP-educated mice after treatment of DMSO or doxorubicin (cumulative dose of 25 mg/kg) as described in (**a**). LVIDd, left ventricular internal dimension at end diastole. LVIDs, left ventricular internal dimension at end systole. EF, ejection fraction. FS, fractional shortening. *P* values were determined by the multiple unpaired *t*-test and two-tailed, unpaired Student's *t*-test. NS, not significant. Data are represented as mean ± s.e.m. An error was made for the statistical test used in (**b**). The correct test should have been the two-way ANOVA with Fisher's LSD test, and this correction was included in the second revision.

5. The authors found tumor-derived EVPs induced fatty liver and decreased drug metabolism. Is this fatty liver associated with decreased drug metabolism or tumor-derived EVPs can decrease drug metabolism independently of fatty liver?

Authors: We thank the reviewer for this insightful comment. As mentioned above, we treated primary hepatocytes with TNFα, and found that TNFα treatment was sufficient to induce lipid droplet accumulation and suppress drug metabolism-associated *Cyp* enzyme gene expression in primary hepatocytes (**Response to Reviewers Figure 21a**,**b**). TNFα treated hepatocytes were also subjected to RNA-seq, and Gene set enrichment analysis (GSEA) revealed that the Drug Metabolism Cytochrome P450 signature was significantly downregulated in hepatocytes after TNFα treatment (**Response to Reviewers Figure 21c**). Interestingly, TNFα blockade not only dramatically reduced fatty liver generation (**Response to Reviewers Figure 21d**,**e**), but also rescued *Cyp* gene expression in the livers of tumor-bearing and tumor EVP- educated mice (**Response to Reviewers Figure 21f**,**g**). Furthermore, the analysis of drug metabolism in precision-cut liver slices demonstrated that TNFα blockade was sufficient to rescue drug metabolism in liver slices from tumor-bearing mice and tumor EVP-treated precision-cut liver slices after anti-TNFαtreatment (**Response to Reviewers Figure 21h,i**). While it is difficult to dissociate fatty liver and drug metabolism, prior studies have indeed shown that fatty liver disease impairs drug metabolism by Cytochrome P450 enzymes (Cobbina and Akhlaghi, 2017; Woolsey *et al.*, 2015). Taken together, our findings indicate that fatty liver disease and impaired drug metabolism are mechanistically interconnected and are both regulated by the pro-inflammatory cytokine TNFα.

References:

Bagdasaryan, A.A., Chubarev, V.N., Smolyarchuk, E.A., Drozdov, V.N., Krasnyuk, II, Liu, J., Fan, R., Tse, E., Shikh, E.V., and Sukocheva, O.A. (2022). Pharmacogenetics of Drug Metabolism: The Role of Gene Polymorphism in the Regulation of Doxorubicin Safety and Efficacy. Cancers (Basel) *14*. 10.3390/cancers14215436.

Bobrie, A., Krumeich, S., Reyal, F., Recchi, C., Moita, L.F., Seabra, M.C., Ostrowski, M., and Thery, C. (2012). Rab27a supports exosome-dependent and -independent mechanisms that modify the tumor

microenvironment and can promote tumor progression. Cancer Res *72*, 4920-4930. 10.1158/0008-5472.CAN-12-0925.
Burd, C.E., Liu, W., Huynh, M.V., Waqas, M.A., Gillahan, J.E., Clark, K.S., Fu, K., Martin, B.L., Jeck, W.R., Souroullas, G.P., et al. (2014). Mutation-specific RAS oncogenicity explains NRAS codon 61 selection in melanoma. Cancer Discov *4*, 1418-1429. 10.1158/2159-8290.CD-14-0729.
Cawthorn, W.P., Heyd, F., Hegyi, K., and Sethi, J.K. (2007). Tumour necrosis factor-alpha inhibits adipogenesis via a beta-catenin/TCF4(TCF7L2)-dependent pathway. Cell Death Differ *14*, 1361-1373. 10.1038/sj.cdd.4402127.
Cobbina, E., and Akhlaghi, F. (2017). Non-alcoholic fatty liver disease (NAFLD) - pathogenesis, classification, and effect on drug metabolizing enzymes and transporters. Drug Metab Rev *49*, 197-211. 10.1080/03602532.2017.1293683.
He, X.Y., Ng, D., and Egeblad, M. (2022). Caught in a Web: Emerging Roles of Neutrophil Extracellular Traps in Cancer. Annu Rev Canc Biol *6*, 223-243. 10.1146/annurev-cancerbio-080421-015537.
Hoshino, A., Kim, H.S., Bojmar, L., Gyan, K.E., Cioffi, M., Hernandez, J., Zambirinis, C.P., Rodrigues, G., Molina, H., Heissel, S., et al. (2020). Extracellular Vesicle and Particle Biomarkers Define Multiple Human Cancers. Cell *182*, 1044-1061 e1018. 10.1016/j.cell.2020.07.009.
Huby, T., and Gautier, E.L. (2022). Immune cell-mediated features of non-alcoholic steatohepatitis. Nat Rev Immunol *22*, 429-443. 10.1038/s41577-021-00639-3.
Juhling, F., Hamdane, N., Crouchet, E., Li, S., El Saghire, H., Mukherji, A., Fujiwara, N., Oudot, M.A., Thumann, C., Saviano, A., et al. (2021). Targeting clinical epigenetic reprogramming for chemoprevention of metabolic and viral hepatocellular carcinoma. Gut *70*, 157-169. 10.1136/gutjnl-2019-318918.
Lancaster, G.I., Langley, K.G., Berglund, N.A., Kammoun, H.L., Reibe, S., Estevez, E., Weir, J., Mellett, N.A., Pernes, G., Conway, J.R.W., et al. (2018). Evidence that TLR4 Is Not a Receptor for Saturated Fatty Acids but Mediates Lipid-Induced Inflammation by Reprogramming Macrophage Metabolism. Cell Metab *27*, 1096-1110 e1095. 10.1016/j.cmet.2018.03.014.
Lewis, I.J., Nooij, M.A., Whelan, J., Sydes, M.R., Grimer, R., Hogendoorn, P.C., Memon, M.A., Weeden, S., Uscinska, B.M., van Glabbeke, M., et al. (2007). Improvement in histologic response but not survival in osteosarcoma patients treated with intensified chemotherapy: a randomized phase III trial of the European Osteosarcoma Intergroup. J Natl Cancer Inst *99*, 112-128. 10.1093/jnci/djk015.
Maddipati, R., and Stanger, B.Z. (2015). Pancreatic Cancer Metastases Harbor Evidence of Polyclonality. Cancer Discov *5*, 1086-1097. 10.1158/2159-8290.CD-15-0120.
Mu, X., Agarwal, R., March, D., Rothenberg, A., Voigt, C., Tebbets, J., Huard, J., and Weiss, K. (2016). Notch Signaling Mediates Skeletal Muscle Atrophy in Cancer Cachexia Caused by Osteosarcoma. Sarcoma *2016*, 3758162. 10.1155/2016/3758162.
Ostrowski, M., Carmo, N.B., Krumeich, S., Fanget, I., Raposo, G., Savina, A., Moita, C.F., Schauer, K., Hume, A.N., Freitas, R.P., et al. (2010). Rab27a and Rab27b control different steps of the exosome secretion pathway. Nat Cell Biol *12*, 19-30; sup pp 11-13. 10.1038/ncb2000.
Park, J., Wysocki, R.W., Amoozgar, Z., Maiorino, L., Fein, M.R., Jorns, J., Schott, A.F., Kinugasa-Katayama, Y., Lee, Y., Won, N.H., et al. (2016). Cancer cells induce metastasis-supporting neutrophil extracellular DNA traps. Sci Transl Med *8*, 361ra138. 10.1126/scitranslmed.aag1711.
Peinado, H., Aleckovic, M., Lavotshkin, S., Matei, I., Costa-Silva, B., Moreno-Bueno, G., Hergueta-Redondo, M., Williams, C., Garcia-Santos, G., Ghajar, C., et al. (2012). Melanoma exosomes educate bone marrow progenitor cells toward a pro-metastatic phenotype through MET. Nat Med *18*, 883-891. 10.1038/nm.2753.
Rau, M., and Geier, A. (2021). An update on drug development for the treatment of nonalcoholic fatty liver disease - from ongoing clinical trials to future therapy. Expert Rev Clin Pharmacol *14*, 333-340. 10.1080/17512433.2021.1884068.

Reid, J.M., Kuffel, M.J., Miller, J.K., Rios, R., and Ames, M.M. (1999). Metabolic activation of dacarbazine by human cytochromes P450: the role of CYP1A1, CYP1A2, and CYP2E1. Clin Cancer Res *5*, 2192-2197.
Sharma, P., Ludwig, S., Muller, L., Hong, C.S., Kirkwood, J.M., Ferrone, S., and Whiteside, T.L. (2018). Immunoaffinity-based isolation of melanoma cell-derived exosomes from plasma of patients with melanoma. J Extracell Vesicles *7*, 1435138. 10.1080/20013078.2018.1435138.
Skat-Rordam, J., Ipsen, D.H., Seemann, S.E., Latta, M., Lykkesfeldt, J., and Tveden-Nyborg, P. (2021). Modelling Nonalcoholic Steatohepatitis In Vivo-A Close Transcriptomic Similarity Supports the Guinea Pig Disease Model. Biomedicines *9*. 10.3390/biomedicines9091198.
Suzuki, T., Von Haehling, S., and Springer, J. (2020). Promising models for cancer-induced cachexia drug discovery. Expert Opin Drug Discov *15*, 627-637. 10.1080/17460441.2020.1724954.
Voltarelli, F.A., Frajacomo, F.T., Padilha, C.S., Testa, M.T.J., Cella, P.S., Ribeiro, D.F., de Oliveira, D.X., Veronez, L.C., Bisson, G.S., Moura, F.A., and Deminice, R. (2017). Syngeneic B16F10 Melanoma Causes Cachexia and Impaired Skeletal Muscle Strength and Locomotor Activity in Mice. Front Physiol *8*, 715. 10.3389/fphys.2017.00715.
Woolsey, S.J., Mansell, S.E., Kim, R.B., Tirona, R.G., and Beaton, M.D. (2015). CYP3A Activity and Expression in Nonalcoholic Fatty Liver Disease. Drug Metab Dispos *43*, 1484-1490. 10.1124/dmd.115.065979.
Xie, Z., Gao, Y., Ho, C., Li, L., Jin, C., Wang, X., Zou, C., Mao, Y., Wang, X., Li, Q., et al. (2022). Exosome-delivered CD44v6/C1QBP complex drives pancreatic cancer liver metastasis by promoting fibrotic liver microenvironment. Gut *71*, 568-579. 10.1136/gutjnl-2020-323014.
Zhang, H., Deng, T., Liu, R., Bai, M., Zhou, L., Wang, X., Li, S., Wang, X., Yang, H., Li, J., et al. (2017). Exosome-delivered EGFR regulates liver microenvironment to promote gastric cancer liver metastasis. Nat Commun *8*, 15016. 10.1038/ncomms15016.
Zhang, H., Freitas, D., Kim, H.S., Fabijanic, K., Li, Z., Chen, H., Mark, M.T., Molina, H., Martin, A.B., Bojmar, L., et al. (2018). Identification of distinct nanoparticles and subsets of extracellular vesicles by asymmetric flow field-flow fractionation. Nat Cell Biol *20*, 332-343. 10.1038/s41556-018-0040-4.
Zhang, H., and Lyden, D. (2019). Asymmetric-flow field-flow fractionation technology for exomere and small extracellular vesicle separation and characterization. Nat Protoc *14*, 1027-1053. 10.1038/s41596-019-0126-x.
Zhang, M., Zhang, Y., Jiao, X., Lai, L., Qian, Y., Sun, B., and Yang, W. (2022). Identification and validation of immune related core transcription factors GTF2I in NAFLD. PeerJ *10*, e13735. 10.7717/peerj.13735.

Reviewer Reports on the First Revision:

Referee #1 (Remarks to the Author):

The revised study by Wang et al includes extensive additions, new experiments and thorough clarifications that, taken together, largely resolve the questions raised in the prior review and add significantly to the appeal of this non-orthodox and extremely interesting paper. Time will tell whether the generality of authors' findings will hold up in the clinic in the case of wider spectrum (all) cancers, but the very notion that not just metastasis, but liver degeneration (NAFLD) are systemic consequences of cancer and cancer-related EVP is fascinating, and sets the stage for years of important research. During the review process the sincerity of the authors lead to some true nuggets, some outside of the main narrative. For example, the mysterious origin of exomeres is at least partially illuminated by their link to Rab27a-mediated export, which is truly interesting and has been documented in the course of revisions. While one can always multiply questions and debate fine points with the authors, this reviewer feels that the study and its revisions are essentially and satisfactorily completed.

Referee #2 (Remarks to the Author):

The authors have satisfactorily addressed my questions. The revised manuscript has significantly improved and clarified several novel concepts introduced in this manuscript. The study provides insights into EVP's new role in reprogramming liver metabolism, conditions that generate PMN vs. fatty liver formation, and the link to chemotherapy-related side effects. The revised manuscript has strengthened these claims by providing data from additional mouse models and patient samples, which also provides clinical relevance.

Referee #3 (Remarks to the Author):

The authors extensively revised the paper by adding a number of new data experimentally. The comments are basically addressed very well, but this reviewer felt some statements are overstated, and has a few minor comments.

1. This reviewer is confused about hepatic lipid accumulation data in the KPC mice (Extended Data Fig. 2k) and PDAC patient data (Fig.1j), and their related discussion on l.531 "Interestingly, our PDAC mouse model and patient data suggest that fatty liver and PMN formation are exclusive of each other, since PMN livers of PDAC bearing mice were not fatty and liver metastasis did not develop in PDAC patients with fatty liver.". First, does EVP-induced fatty liver depend on cancer type? Melanoma caused fatty liver, but not PDAC in mice. If this is the case, human data cannot be explained well. If cancer type is associated with fatty liver, how? Is there any good explanation? Second, is the statement "liver metastasis did not develop in PDAC patients with fatty liver." true? Is there any evidence that PDAC patients with fatty liver do not develop liver metastasis? The clinical

samples from this manuscript cannot conclude it. This statement is overstated.
2. Together with their animal studies, the authors interpreted fatty liver data from the patients (Fig.1j, Supplementary Table 5b, Extended Data Fig.2l) that cancer EVP causes fatty liver in PDAC patients. However, as mentioned by the authors, recent clinical studies showed fatty liver affects not only liver cancer but also promotes other primary cancers (and could be metastasis). Thus, it may not exclude the possibility of more pre-existing fatty liver in PDAC patients. Adding some discussions may be helpful.
3. Regarding the relationship between fatty liver and decreased drug metabolism, this reviewer agrees that TNFa mediates both. However, the statement could make an impression that TNFa-induced decreased drug metabolism is the cause of fatty liver. I believe this cannot be led by the data (even from the previous literature). Improvement of the statement is recommended.
4. Regarding chemotoxicity, the authors measured blood counts and cardiotoxicity. These data are very good. What is hepatotoxicity by measuring liver enzyme levels? It may not be explained well because cancer-EVP causes fatty liver, which may affect blood liver enzyme levels anyway.

Author Rebuttals to First Revision:

Referees' comments:

Referee #1 (Remarks to the Author):

The revised study by Wang et al includes extensive additions, new experiments and thorough clarifications that, taken together, largely resolve the questions raised in the prior review and add significantly to the appeal of this non-orthodox and extremely interesting paper. Time will tell whether the generality of authors' findings will hold up in the clinic in the case of wider spectrum (all) cancers, but the very notion that not just metastasis, but liver degeneration (NAFLD) are systemic consequences of cancer and cancer-related EVP is fascinating, and sets the stage for years of important research. During the review process the sincerity of the authors lead to some true nuggets, some outside of the main narrative. For example, the mysterious origin of exomeres is at least partially illuminated by their link to Rab27a-mediated export, which is truly interesting and has been documented in the course of revisions. While one can always multiply questions and debate fine points with the authors, this reviewer feels that the study and its revisions are essentially and satisfactorily completed.

Authors: We thank the reviewer for the support of our revised manuscript.

Referee #2 (Remarks to the Author):

The authors have satisfactorily addressed my questions. The revised manuscript has significantly improved and clarified several novel concepts introduced in this manuscript. The study provides insights into EVP's new role in reprogramming liver metabolism, conditions that generate PMN vs. fatty liver formation, and the link to chemotherapy-related side effects. The revised manuscript has strengthened these claims by providing data from additional mouse models and patient samples, which also provides clinical relevance.

Authors: We thank the reviewer for the support of our revised manuscript.

Referee #3 (Remarks to the Author):

The authors extensively revised the paper by adding a number of new data experimentally. The comments are basically addressed very well, but this reviewer felt some statements are overstated, and has a few minor comments.

Authors: We thank the reviewer for the positive assessment of our revised manuscript.

1. This reviewer is confused about hepatic lipid accumulation data in the KPC mice (Extended Data Fig. 2k) and PDAC patient data (Fig.1j), and their related discussion on l.531 "Interestingly, our PDAC mouse model and patient data suggest that fatty liver and PMN formation are exclusive of each other, since PMN livers of PDAC bearing mice were not fatty and liver metastasis did not develop in PDAC patients with fatty liver.". First, does EVP-induced fatty liver depend on cancer type? Melanoma caused fatty liver, but not PDAC in mice. If this is the case, human data cannot be explained well. If cancer type is associated with fatty liver, how? Is there any good explanation? Second, is the statement "liver metastasis did not develop in PDAC patients with fatty liver." true? Is there any evidence that PDAC

patients with fatty liver do not develop liver metastasis? The clinical samples from this manuscript cannot conclude it. This statement is overstated.

Authors: We apologize for the lack of clarity in our interpretation, and we have revised our statements to improve clarity. For the current study, we investigated the alterations in the "educated" liver which is distinct from the "pre-metastatic" liver. We have chosen to focus on murine models of melanoma, osteosarcoma and breast cancer to investigate the effects of tumor-derived EVPs on liver function specifically because these models *do not* develop a liver PMN or liver metastasis, and the metastatic dissemination is exclusively extrahepatic. We reasoned that in these models which do not develop hepatic metastasis despite EVP uptake, the functional reprograming of the liver "educated" by EVPs must be distinct from that observed in murine models that *do* develop liver metastasis, such as PDAC. As we reported in our revised manuscript, in the KPC pancreatic cancer model, we observed the formation of "pre-metastatic" livers which were associated with the absence of fatty liver disease.

Based on evaluation of several murine models that do not develop liver metastasis (as well as corresponding human cell line and PDX models) and comparison with murine PDAC models that do develop liver metastasis, we found that the capacity of EVPs to induce fatty liver is inversely correlated with the presence of a PMN.

Redacted text

Therefore, we postulate that cargo of EVPs released by tumors that induce hepatic metastasis promotes liver PMN formation, while EVPs released by tumors that promote extrahepatic metastasis, may promote fatty liver formation (via palmitic acid cargo). In other words, it is not the cancer type *per se*, but the propensity of a given individual cancer to metastasize or not to the liver that dictates PMN versus fatty liver formation. To avoid confusion, we modified the statement in the manuscript to: "Our data comparing livers from PDAC mouse models with hepatic metastases versus mouse models and patients with extrahepatic metastases suggest that fatty liver generation and pre-metastatic liver formation are inversely correlated, and may thus be regulated by different mechanisms, which will require further investigation." (On page 17, line 516-519).

Redacted text and figure

2. Together with their animal studies, the authors interpreted fatty liver data from the patients (Fig.1j, Supplementary Table 5b, Extended Data Fig.2l) that cancer EVP causes fatty liver in PDAC patients. However, as mentioned by the authors, recent clinical studies showed fatty liver affects not only liver cancer but also promotes other primary cancers (and could be metastasis). Thus, it may not exclude the possibility of more pre-existing fatty liver in PDAC patients. Adding some discussions may be helpful.

Authors: We agree with the reviewer that our clinical data cannot exclude the possibility of pre-existing fatty liver in PDAC patients. Indeed, there is limited and potentially contradictory data on the association between NAFLD and PDAC incidence. Two recent clinical studies suggest that presence of NAFLD is associated with an increased risk of PDAC development compared to absence of NAFLD (Allen et al., 2019; Park et al., 2022), while others reported modest or null associations (Kim et al., 2018; Simon et al., 2021). However, those studies have a selection bias as the patients with cancers diagnosed prior to documentation of NAFLD were excluded (Allen *et al.*, 2019; Kim *et al.*, 2018; Park *et al.*, 2022; Simon *et al.*, 2021), thus it is possible that PDAC may also cause fatty liver. Furthermore, these studies did not take into account whether the patients develop hepatic or extrahepatic metastasis. Based on our study, we hypothesize that NAFLD can protect the liver from metastasis (while likely promoting primary cancer (PDAC and others) and/or metastasis elsewhere).

Therefore, to address the reviewer's request, we expanded the discussion of this point as shown below:

"Although our data suggest a functional role for tumor-derived EVPs in fatty liver generation, it does not exclude the possibility of pre-existing fatty liver in PDAC patients. Indeed, there is limited and potentially contradictory data on the association between NAFLD and PDAC incidence. Two recent clinical studies suggest that presence of NAFLD is associated with an increased risk of PDAC development compared to absence of NAFLD (Allen *et al.*, 2019; Park *et al.*, 2022), while others reported modest or null associations (Kim *et al.*, 2018; Simon *et al.*, 2021). One point to make is that those studies have a selection bias as the patients with cancers diagnosed prior to documentation of NAFLD were excluded (Allen *et al.*, 2019; Kim *et al.*, 2018; Park *et al.*, 2022; Simon *et al.*, 2021), thus it is possible that PDAC may also cause fatty liver. Furthermore, those studies did not take into account whether the patients develop hepatic or extrahepatic metastasis. Based on our study, we hypothesize that NAFLD may protect liver from metastasis, and tumor EVP-induced liver metabolic dysfunction in cancer patients needs to be further investigated." (On page 17-18, line 540-550).

3. Regarding the relationship between fatty liver and decreased drug metabolism, this reviewer agrees that TNFa mediates both. However, the statement could make an impression that TNFa-induced decreased drug metabolism is the cause of fatty liver. I believe this cannot be led by the data (even from the previous literature). Improvement of the statement is recommended.

Authors: We thank the reviewer for this suggestion. We have modified statements throughout the manuscript:
Line 73, change "by tumor EVP-induced fatty liver" to "by tumor EVP education"
Line 423, delete "to generate the fatty liver"
Line 429, delete "bearing fatty livers"
Line 434, delete "to induce fatty liver formation"
Line 440, delete "with fatty livers"
Line 442, delete "and fatty liver generation"
Line 533-534, change "Our study demonstrates that fatty liver interferes with the hepatic metabolic function and drug metabolism" to "Our study demonstrates that tumor EVPs induce fatty liver generation and interfere with the hepatic metabolic function and drug metabolism."

4. Regarding chemotoxicity, the authors measured blood counts and cardiotoxicity. These data are very good. What is hepatotoxicity by measuring liver enzyme levels? It may not be explained well because cancer-EVP causes fatty liver, which may affect blood liver enzyme levels anyway.

Authors: Based on the reviewer's comment, we measured liver enzymes (alanine transaminase [ALT], aspartate transaminase [AST]) and lactate dehydrogenase [LDH] in the serum of PBS- or EVP- educated mice that were treated with chemotherapy as described in the manuscript (**Figure 6g,h** and **Extended data Figure 10c**).

In the melanoma model, dacarbazine treatment did not induce changes in ALT, AST, or LDH levels in either control PBS or B16F10-CL-EVP educated mice (**Response to reviewers Figure 2a**, for reviewers only), indicating there is no or limited liver toxicity induced by dacarbazine treatment in B16F10-CL-EVP-educated mice.

In the osteosarcoma model, doxorubicin treatment tended to induce elevation of ALT, AST, and LDH levels in the serum of all PBS, osteoblast-EVP and K7M2-CL-EVP-educated mice, compared to DMSO treatment (**Response to reviewers Figure 2b**, for reviewers only). Strikingly, doxorubicin induced the highest ALT and LDH levels in the serum of K7M2-CL-EVP educated mice, compared to control PBS or osteoblast-EVP-

educated mice. ALT elevation is often the most sensitive enzyme reflecting liver damage (Giannini et al., 2005; Newsome et al., 2018). LDH is an acute phase reactant often elevated in the serum due to liver or cardiac injury (Farhana and Lappin, 2022). Thus, our results suggest that K7M2-CL-EVP education may enhance doxorubicin-induced hepatotoxicity.

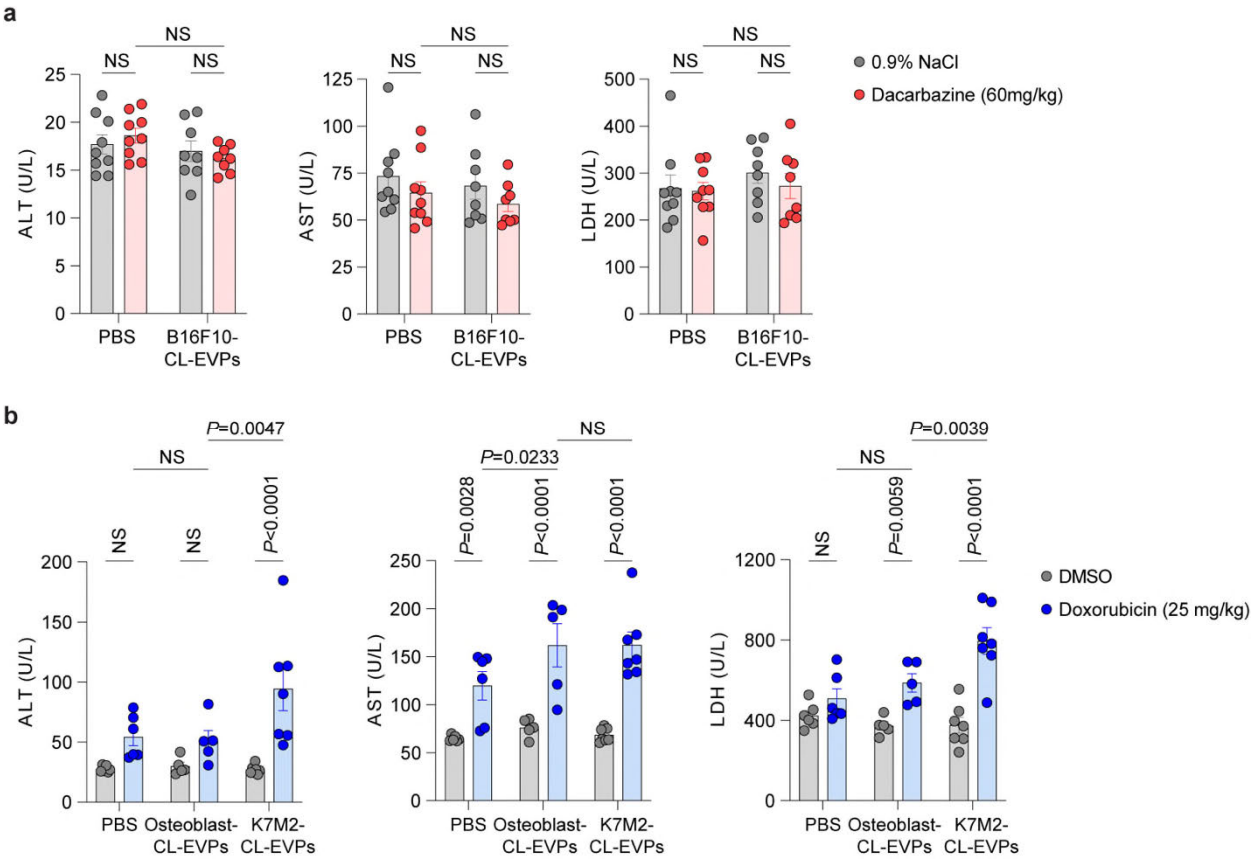

Response to reviewers Figure 2. Liver enzyme levels in the blood of EVP-educated mice after treatment with chemotherapeutic drugs. a, Statistical analysis of ALT, AST, and LDH levels in the serum of PBS- or B16F10-CL-EVP-educated mice after treatment with dacarbazine (60 mg/kg) or 0.9% NaCl. n=9 mice for PBS groups and n=8 mice for B16F10-CL-EVP groups. **b**, Statistical analysis of ALT, AST, and LDH levels in the serum of PBS-, or osteoblast-EVP-, or K7M2-CL-EVP-educated mice after treatment with doxorubicin (cumulative dose of 25 mg/kg) or DMSO. n=6 mice for PBS groups, n=5 mice for osteoblast-EVP groups, and n=7 mice for K7M2-CL-EVP groups. *P* values were determined by two-way ANOVA followed with Fisher's LSD test. NS, not significant. Data are represented as mean ± s.e.m.

References

Allen, A.M., Hicks, S.B., Mara, K.C., Larson, J.J., and Therneau, T.M. (2019). The risk of incident extrahepatic cancers is higher in non-alcoholic fatty liver disease than obesity - A longitudinal cohort study. J Hepatol *71*, 1229-1236. DOI 10.1016/j.jhep.2019.08.018.

Costa-Silva, B., Aiello, N.M., Ocean, A.J., Singh, S., Zhang, H., Thakur, B.K., Becker, A., Hoshino, A., Mark, M.T., Molina, H., et al. (2015). Pancreatic cancer exosomes initiate pre-metastatic niche formation in the liver. Nat Cell Biol *17*, 816-826. 10.1038/ncb3169.

Farhana, A., and Lappin, S.L. (2022). Biochemistry, Lactate Dehydrogenase. In StatPearls.

Giannini, E.G., Testa, R., and Savarino, V. (2005). Liver enzyme alteration: a guide for clinicians. CMAJ *172*, 367-379. 10.1503/cmaj.1040752.
Kim, G.A., Lee, H.C., Choe, J., Kim, M.J., Lee, M.J., Chang, H.S., Bae, I.Y., Kim, H.K., An, J., Shim, J.H., et al. (2018). Association between non-alcoholic fatty liver disease and cancer incidence rate. J Hepatol *68*, 140-146. DOI 10.1016/j.jhep.2017.09.012.
Newsome, P.N., Cramb, R., Davison, S.M., Dillon, J.F., Foulerton, M., Godfrey, E.M., Hall, R., Harrower, U., Hudson, M., Langford, A., et al. (2018). Guidelines on the management of abnormal liver blood tests. Gut *67*, 6-19. 10.1136/gutjnl-2017-314924.
Park, J.H., Hong, J.Y., Han, K., Kang, W., and Park, J.K. (2022). Increased risk of pancreatic cancer in individuals with non-alcoholic fatty liver disease. Sci Rep *12*, 10681. 10.1038/s41598-022-14856-w.
Simon, T.G., Roelstraete, B., Sharma, R., Khalili, H., Hagstrom, H., and Ludvigsson, J.F. (2021). Cancer Risk in Patients With Biopsy-Confirmed Nonalcoholic Fatty Liver Disease: A Population-Based Cohort Study. Hepatology *74*, 2410-2423. 10.1002/hep.31845.

Reviewer Reports on the Second Revision:

Referee #3 (Remarks to the Author):

Thank you, authors, for the clarifications. This reviewer does not have any further comments.